MULTI-OBJECTIVE OPTIMAL SIZING AND OPERATION CONTROL OF MICROGRID-CONNECTED BATTERYLESS ENERGY SYSTEM UNDER TIME OF USE TARIFF

KASEREKA NDWALI

MASTER OF SCIENCE
(Mechatronic Engineering)

JOMO KENYATTA UNIVERSITY OF AGRICULTURE AND TECHNOLOGY

2020

Multi-Objective Optimal Sizing and Operation Control of Microgrid-Connected Batteryless Energy System Under Time of Use Tariff

Kasereka Ndwali

A thesis Submitted in Partial Fulfillment of the Requirements for the Degree of Master of Science in Mechatronic Engineering in the Jomo Kenyatta University of Agriculture and Technology

2020

DECLARATION

This thesis is my original work and has not been presented for a degree in any other university.

Signature.. Date............./................/..................

Kasereka Ndwali

This thesis has been submitted for examination with our approval as university supervisors:

Signature.. Date............./................/..................

Dr. -Ing. Jackson G. Njiri,PhD

JKUAT,Kenya

Signature.. Date............./................/..................

Dr. -Eng. Evan M. Wanjiru,PhD

JKUAT,Kenya

DEDICATION

To Almighty God for the strength, patience, wisdom, and many blessings bestowed upon me.

To my parents, Badiona Tsongo Sivihumbwa and Adileda Kavira Nziavake, for all the sacrifices, love, supports and prayers you have continually made.

My siblings Patient, Lucien, Rachel, Grace, Emmanuel, Christian and Christiana for you supports.

To Dr Eraston Kambale Kighoma for your encouragements, inspirations and prayers.

ACKNOWLEDGMENT

The achievement of this research would not have been possible without the contributions of many people, to whom I wish to express my gratefulness.

I am deeply grateful to my supervisors Dr.-Ing Jackson G. Njiri and Dr. -Eng Evan M. Wanjiru for their continuous guidance, advices, inspirations and patience throughout the duration of my thesis research. Their valuable ideas help me to generate and produce a good research findings.

I would like to show my deepest gratitude to my family, especially to my parents Badiona Tsongo Sivihumbwa and Adileda Kavira Nziavake, the one to whom I owe all the success in my life. No words can express my gratitude to them, I pray the Almighty God to bless and reward them. I will always love you.

I would like to convey my gratefulness to the Center for Intercultural Missions and Research (CIMR), for their supports.

My appreciation is also extended to my fellow classmates, Patrick Kipkosgei, Leila Mbagaya, Maurine Naliaka, Claver Nsanzumuhire, David Ngibwini, Edwin Kipchirchir, John Chege, and Sylvester Njorogue. Thanks for the great moments we shared out together.

TABLE OF CONTENTS

LIST OF TABLES

LIST OF FIGURES

LIST OF ABBREVIATIONS

AC :Alternating Current

AI :Artificial Intelligence

ANN :Artificial Neural Network

BESS :Battery Energy Storage System

DC :Direct Current

DERs :Distributed Energy Resources

DG :Diesel Generator

DR :Demand Response

DSM :Demand Side Management

EMPC :Economic Model Predictive Control

FLC :Fuzzy Logic Control

GA :Genetic Algorithm

HOMER :Hybrid Optimization Model Electric Renewable

HVAC :Heating, Ventilation and Air Conditioning

IM :Intermittent Mode

ICM :Intermittent Connected Mode

KF :Kalman Filter

LP :Linear Programming

LPSP :Loss of Power Supply Probability

LQI :Linear Quadratic Integrator

LQR :Linear Quadratic Regulator

MILP :Mixed Integer Linear Programming

MIMO :Multi-Input Multi-Output

MPC :Model Predictive Control

PCC :Point of Common Coupling

PID :Proportional Integral Derivative

PPA :Power Purchase Agreement

PSO :Particle Swarm Optimization

PV :Photovoltaic

SISO :Single Input Single Output

TLCC :Total Life Cycle Cost

TOU :Time of Use

ABSTRACT

Many countries are exponentially faced with high demand of electricity due to factors such as high living standards, industrialization, population growth, among other factors. As a result, the integration of renewable energy sources at distribution power level systems has increased, mainly because of global warming concerns. Modern power systems are geared towards distributed energy resources (DERs) at the distribution level networks. In this sense, microgrids are the main core infrastructure of today's modern power system. Microgrids consists of interconnection of distributed energy resources such as renewable energy sources, storage energy systems, diesel generators, and loads. In recent years, microgrids based on photovoltaic energy system are becoming popular for electrification both for grid-connected mode and isolated mode. However, the deployment of a microgrid photovoltaic system brings many challenges due to stochastic nature of photovoltaic energy source and variability of load demand. This is because power generation must always match the load demand. Therefore, the main issues related to microgrid-connected photovoltaic systems are the optimization design parameters, planning and operation control schemes which seek to minimize or maximize predefined objective functions subject to technical and operational constraints. Importantly, designing a cost-effective microgrid-connected photovoltaic system alongside the dispatching and scheduling the power flows is very crucial in modern power system. Accordingly, this thesis is mainly divided into two major parts namely, optimal sizing of grid-connected photovoltaic batteryless energy system and optimal operation control of microgrid-connected photovoltaic-diesel generator backup energy system. In the first part, a multi-objective optimal sizing grid-connected photovoltaic batteryless system that seeks to determine the most cost-effective photovoltaic (PV) system size that maximizes the reliability requirements while lowering the power

sold to the grid utility. This is because there is no power purchase agreement (PPA) within this jurisdiction. The economic analysis is expressed in terms of total life cycle cost and the microgrid reliability is measured by the loss of power supply probability (LPSP). On the other hand, optimal operation control in conjunction with demand side model (DSM) is carried out to improve the operational efficiency and resilience of microgrid-connected photovoltaic-diesel generator energy system. Time of use tariff (TOU) is the type of DSM strategy considered in this research. Essentially, an open loop optimal and a closed-loop control are suitably designed. The open loop scheme takes into consideration the non-linearity of the diesel generator fuel consumption; and, the FMINCON algorithm in MATLAB is used to carry out the optimization problem. The closed-loop system is based on economic model predictive control (EMPC) solved using linear programming (LP) in OPTI Toolbox. In both open loop and closed-loop strategies, operational efficiency and energy efficiency are considerably improved. Notwithstanding, each of the two control schemes exhibits its pros and cons. On one hand, the open loop optimal control strategy is not complex and is stable. Thus, it is easier and cheaper to implement but cannot handle uncertainties and disturbances within the microgrid energy systems. On the other hand, the closed-loop EMPC strategy is complex and expensive to implement but present great robustness against uncertainties and disturbances. From the results obtained, the optimal number is 354 photovoltaic panels and the total life cycle cost of the system is found to be 191630$ over 25 years lifespan of the project. From the optimal operation control point of view, the daily energy saving is increased up to 52.1 % in intermittent connected mode (ICM) while the diesel energy not delivered increases to 84.8 % in intermittent mode (IM). The results of this thesis are evidently crucial for designers, decision-makers, performances analyzers, and control agents who are struggling with multiple objectives to make appropriate trade-offs for grid-connected photovoltaic systems.

CHAPTER ONE

INTRODUCTION

1.1 Background

Electricity is one of the most important and widely used type of energy all over the world. In fact, it is mainly the core substructure of economic and social activities in the modern society. Conventional power systems include power plants using fossil fuels such as coal and natural gas. They are presently facing challenges of meeting future electricity demand along with greenhouse gases concerns (Adefarati & Bansal, 2017a; M. I. Nwulu et al., 2015). Therefore, conventional power systems need to be restructured in order to meet the continuous growing energy demand (Ekren & Ekren, 2010; Kusakana, 2016b; Nguyen, Nguyen, & Tran, 2015). The distributed energy sources of electricity production based on renewable energy resources such as photovoltaic solar, wind turbine, hydro, among others are becoming popular in enhancing the reliability of energy and operation efficiency of power systems at low level distribution network system in several countries. These renewable energy sources can be integrated in a typical microgrid that mainly contains different distributed energy resources (DERs) (Rawat, Kaushik, & Lamba, 2016).

Microgrid energy systems can operate either in connected mode with the grid utility or autonomous mode in remote area where the extension of the grid utility may present a exorbitant cost. In general, the deployment of the distributed energy resources allows the modern power systems to enable bidirectional power flow (Camacho, Samad, Garcia-Sanz, & Hiskens, 2011; Kiplagat, Wang, & Li, 2011; Nguyen et al., 2015; Tina & Pappalardo, 2009). Moreover, microgrids present some inherent advantages such as: improved reliability, minimum greenhouse gases emissions, saving the cost of energy delivery, improved power quality, among other advantages (Du et al., 2014; N. I. Nwulu & Xia, 2017).

In Kenya, electricity consumption is increasing at a very high rate; Hence, Kenya's vision 2030 projected electrical energy as a key foundation upon which the economic, social, and political pillars of the long-term development strategies will be built (Boampong & Phillips, 2016; Kiplagat et al., 2011). Kenya has to diversify energy generation sources in order to exploit other sources of energy generation and reduce the stress on the grid utility (Boampong & Phillips, 2016; Kiplagat et al., 2011). Among distributed energy resources, photovoltaic solar energy systems have gained attractive interest due to benefits such as: environmentally friendly, availability, cost-effectiveness, and no noise (Mishra, Ramasubramanian, & Sekhar, 2013). Evidently, Kenya is endowed with abundant solar irradiation that remains unexploited for photovoltaic solar energy generations. Importantly, the country can harness grid-connected photovoltaic system in urban areas where the grid utility is readily available. This can significantly lower the burden of the utility grid and ensure that there is sufficient margin of supply in any generation plants (Kenya & Africa, 2016a; Tigabu, 2016a).

The principal drawbacks of photovoltaic energy systems is intermittent and unreliable characteristics such as: seasonal and weather conditions; hence, they require effective interfaces to mitigate these drawbacks. They are operated in conjunction with battery energy storage for small scale or residential applications in order to improve the reliability of microgrid energy system. Although, grid connected photovoltaic system present many benefits, they exhibit a high cost due to the connection of energy storage systems for large scale applications (Alramlawi, Gabash, Mohagheghi, & Li, 2018b). Energy storage systems present high capital cost, operating & maintenance, and replacement costs (García-Triviño et al., 2015; Tsuanyo, Azoumah, Aussel, & Neveu, 2015). As stated by phiri et al., Wu et al. in (Phiri & Kusakana, 2016; Wu, Tazvinga, & Xia, 2015), grid-connected photovoltaic do not require battery storage energy system because the surplus photovoltaic energy can be sold back to the grid. Therefore, microgrid system reliability is reduced when the storage energy systems are not considered in the design process. To ensure reliability, diesel generators are often used as backup system to guarantee uninterrupted power supply for commercial and industrial applications. They have been considered as cost-effective systems in lieu of storage energy systems in large scale applications such as industrial & commercial facilities (Elmitwally & Rashed, 2010). However, diesel generators can be operated at any time because they do not depend on the weather conditions as apposed to renewable energy sources. Diesel generators present negative environmental impacts and high operation & maintenance (O&M) costs.

Notwithstanding, microgrid-connected photovoltaic systems exhibit numerous challenges relating to optimal design, planning, and operation control this is caused by the intermittent nature of photovoltaic, unscheduled power outages, real time variation of load demand at each time and bidirectional transmissions power (Adefarati & Bansal, 2017a). It is therefore important to optimize the microgrid-connected photovoltaic systems. In this perspective, microgrid-connected photovoltaic systems are receiving particular attention with the development of smart grids technologies in modern power systems. Systematically, microgrid system designers, decisions makers, and operators are either maximizing or minimizing some predetermined objective functions in order to maximize profit and reliability as well as minimizing operation cost and greenhouse gases emissions, among others. To design efficient, reliable and cost effective microgrid systems, the optimal sizing and dynamic operation control must be carried out to minimize production costs and maximize efficiency and resiliency of microgrid energy systems (Borhanazad, Mekhilef, Ganapathy, Modiri-Delshad, & Mirtaheri, 2014; Fathy, 2016).

In this study, efficient and innovative optimization algorithms are developed to deal with the challenges for microgrid-connected photovoltaic batteryless systems.

The optimal sizing approach seeks to design the microgrid photovoltaic batteryless system that is cost-effective while at the same time guaranteeing the reliability requirement. The optimal sizing minimizes the Total Life Cycle Cost (TLCC) and the grid energy while maximizing the reliability expressed in terms of Loss of Power Supply Probability (LPSP). Furthermore, the optimal operation control along with the demand side management strategy seeks to efficiently and economically manage the available distributed energy resources with diesel generator as backup energy system. The objective function is to minimize the cost of energy purchased from the grid utility and the fuel consumption cost of the diesel generator while taking into account the constraints related to controllable variables. The time of use (TOU) tariff for Commercial & Industrial 1 (C&I 1) in Kenya is the classic demand side management (DSM) used in this thesis.

1.2 Motivation and problem statement

The process of designing, planning, and operating the microgrid- connected photovoltaic energy system is always a complex one, this is because of ensuring the dynamic balance of the power demand and supply. The ever-increasing demand of electricity has strained the traditional electrical power system leading to frequent power outage. As a result, unreliable supply of electricity by main grid utilities has forced many customers of commercial and industrial facilities to rely on diesel generators as backup system. Despite the fact that diesel generators present a cost-effective capital, their operation & maintenance costs are high and they emit greenhouse gases emissions. The incorporation of renewable energy resources can mitigate the negative effects of diesel generator. To address the inherent negative consequences of power outage, grid-connected photovoltaic-diesel backup energy systems are currently playing major role. In this regard, the deployment of microgrid photovoltaic-diesel backup energy systems presents new challenges which are the intermittent nature of photovoltaic energy sources, variability of loads demand, and unscheduled power outages. Importantly, the generated power must always meet the fluctuating load demand at each time within the microgrid. As a result, the optimal sizing and operation control of such dynamic power system is not straightforward due to the dynamic interaction between photovoltaic solar energy, grid utility, and load demand. The interest in this paradigm is to optimize the grid-connected photovoltaic system on the basis of multi-objective approach while guaranteeing the reliability as constraints. To achieve operational and energy efficiency while improving the reliability and resiliency of microgrid, it is important to establish an optimal control strategy under demand side management.

1.3 Objectives

The main objective of this research was to optimally size and develop the optimal operation control strategy of microgrid-connected photovoltaic batteryless energy system. To achieve the main objective, the following specific objectives were accomplished:

1. To size grid-connected photovoltaic batteryless energy system using a multi-objective optimization technique.
2. To develop a constrained open loop optimal control algorithm in order to optimize the control operation of microgrid-connected photovoltaic-diesel generator system under time of use.
3. To develop a closed-loop control based on Economic Model Predictive Control (EMPC) strategy to optimize the control operation of microgrid-connected photovoltaic-diesel generator system under time of use.

1.4 Scope

The deployment of microgrid-connected photovoltaic batteryless systems is growing rapidly to exploit solar as a source of energy and meet future energy demand. This research is carried out at Jomo Kenyatta University of Agriculture and Technology (JKUAT). Jomo Kenyatta University of Agriculture and technology is located in Kenya, Kiambu county, Juja town at -1.099 ° latitude and 37.014 ° longitude. More specifically, the scope of this research is limited to the Engineering workshops at Jomo Kenyatta University of Agriculture and Technology (JKUAT).

1.5 Layout of thesis

This thesis is presented in two broad parts: the optimal sizing and operation control strategy of microgrid-connected photovoltaic with diesel generator backup system. The structure is thus broken out as follows,

Chapter 1 is the introduction. The chapter offers the relevant background information related to the optimal sizing and operation control of microgrid energy systems, the motivation and problem statement, and the objectives of the research. Moreover, the scope and the layout of the thesis are presented in this chapter.

Chapter 2 provides the literature review on optimal sizing and operation control strategies of microgrid energy systems, the theoretical background as well as summary of research gaps.

Chapter 3 presents the multi-objective optimal sizing of microgrid-connected photovoltaic batteryless energy system. A novel and efficient mixed integer linear programming algorithm is developed to find the optimal variables which simultaneously minimize two objective functions namely the total life cycle cost and the grid energy.

Chapter 4 presents an optimal operation control of microgrid-connected photovoltaic-diesel generator backup system under time of use tariff. It considers an open loop control algorithm that minimizes the grid energy cost and the fuel consumption cost while considering constraints between the control variables over 24 hours period.

Chapter 5 presents an economic model predictive control approach microgrid-connected photovoltaic-diesel generator backup under time of use tariff. This advances the previous chapter on the closed loop control based receding horizon control to determine the optimal operation control strategy of the proposed microgrid photovoltaic system.

Chapter 6 provides the conclusion of the research work covered the previous chapters and future research recommendations.

CHAPTER TWO

LITERATURE REVIEW AND THEORETICAL BACKGROUND

Microgrid designers, performance analyzers, decisions makers and operators are faced with numerous challenges concerning optimization of microgrids due to intermittent nature of renewable energy sources, non-linearity of components, variations in power demand, dynamic and extension of grid utility. This chapter provides a critical literature review on optimization sizing and optimal operation control of microgrid energy systems using open loop and closed-loop mechanisms and the theoretical background.

2.1 Types of microgrid energy systems

The increase in demand of electricity and growing environmental concerns, renewable energy sources such as photovoltaic, wind, biomass, and micro hydraulic, which do not emit greenhouse gas are fast becoming common in the distribution power system (Rawat et al., 2016). Among these renewable energy resources, microgrid that consists of photovoltaic solar has gained widespread popularity due to the fact that it is readily available, and environmentally friendly and no noise, among other factors (Sulaiman, Rahman, Musirin, & Shaari, 2011). The microgrid energy system can be used in grid-connected mode and stand alone mode applications (K. Ndwali et al., 2020b).

2.2 Sizing techniques of microgrids and critic

With the development of today's power systems, microgrid photovoltaic systems are used to provide electricity either in autonomous mode for remote areas or grid-connected mode for urban communities to supplement grid utility. Although grid-connected photovoltaic systems are widely installed all over the world, their total life cycle cost (TLCC) is excessively high (Mondol, 2007; Ramli, Hiendro, Sedraoui, & Twaha, 2015; Sulaiman et al., 2011). Several approaches have been conducted to reduce some components of the TLCC which include investment cost, operation and maintenance cost, among others. In particular, studies have been conducted to optimize the size of grid-connected photovoltaic systems and several optimization algorithms have been developed in recent years.

Many studies have been conducted in the optimization of grid-connected photovoltaic systems. In a study conducted by Acakpovi et al. (Acakpovi, Michael, & Majeed, 2017a), Nurunnabi et al. (Nurunnabi, Roy, & Pota, 2019), Ramli et al. (Ramli, Hiendro, Sedraoui, & Twaha, 2015), the authors presented an optimization sizing of microgrid using software simulation tools namely Hybrid Optimization Model Electric Renewable (HOMER) to minimize techno-economic analysis. However, HOMER software is limited since it only minimizes a single objective function namely net present cost. In a research by Khanfara et al. (Khanfara, El Bachtiri, Boussetta, & El Hammoumi, 2018), the authors developed a techno-economic sizing of grid-connected photovoltaic system using sunny design software. The optimization approach includes the quality and price of each component of the installation. Other studies of grid-connected photovoltaic systems dealt with optimal sizing of small scale applications such as residential facilities. In a study conducted by Dulout et al. (Dulout et al., 2017), the authors discussed the optimal sizing of lithium battery storage system to minimize the annual cost of storage system on the basis of enhancing its lifetime. The authors did not investigate the deviation of the battery capacity to the changing of the charging & discharging rate under peukert's law. In a study discussed by Li et al. (J. Li, 2019), an optimal sizing of photovoltaic-battery for residential houses to lower the total annual cost of electricity is explored using genetic algorithm. The authors did not consider the leakage and full charge & discharge capabilities in the modelling of battery energy systems. In another study by Abul et al. Abul'Wafa (2017), the energy storage system is optimized to minimize the operating cost of grid-connected photovoltaic system. The authors found out that when the battery energy system is allowed to discharge its energy up to the minimum charge state at the peak hours, the grid-connected photovoltaic presented excessive financial benefit. However, the energy flow optimization under time of use (TOU) tariff rate can be extended to the TOU of peak demand charging tariff. In a research by Ru et al. (Ru, Kleissl, & Martinez, 2013), energy storage system is optimized to minimize the battery capacity and the net power purchased while lowering the peak electricity purchased from the grid utility. The storage energy system can further be optimized and generalized by considering the stochastic photovoltaic solar generation. In a research carried out by Alhaddad et al. (Alhaddad & Alsaad, 2016), an optimal design of grid-connected photovoltaic system on rooftop area using analytic method is examined. The authors did not investigate the life cost analysis of the grid-connected photovoltaic system.

The optimal sizing of large scale applications for grid-connected photovoltaic energy systems have been carried out as well. In study investigated by Sulaiman et al. (Sulaiman et al., 2011), the optimal sizing of grid-connected photovoltaic system is examined to minimize the net present value using genetic algorithm (GA). However, the optimization sizing did not consider other objectives. In a study by Al-Enezi et al. (Al-Enezi, Sykulski, & Rotaru, 2014), the optimal sizing is investigated to minimize the difference between the electrical energy generation and energy demand using iterative approach. Results indicate that the monthly and yearly averaged solar radiations significantly influence the size of photovoltaic panels and inverter.

In a study by Omar et al. (Omar & Shaari, 2009), the authors examined the optimal sizing of grid-connected photovoltaic system considering polycrystalline cell, monocrystalline cell and thin film cell to minimize the investment cost. In this study, the authors did not consider the hourly variation of solar irradiation to optimize the grid-connected PV system. In a research carried out by al-Maghalseh (Al-Maghalseh, 2019a), an optimization sizing of grid connected and stand-alone photovoltaic system without battery storage to minimize net present value with respect to the voltage profile, power flow, and energy losses Results show a great enhancement in the voltage profile and total energy losses in reference to load demand and energy generation is examined. The reliability assessment was not conducted in this study. In a study by Manoj et al. (Manoj Kumar, Sudhakar, & Samykano, 2017), the authors developed an optimal sizing of a grid-connected photovoltaic system to minimize techno-economic analysis using photovoltaic geographical information system and photovoltaic watt's software. The optimization is on the basis of the annual savings, environmental aspects and payback period. It has been demonstrated that this system can lower the greenhouse gases emissions, carbon footprint and enhance sustainable green campus initiative. The optimal tilt angle of the photovoltaic panels in the location was not taken into consideration.

Other researchers dealt with the optimization of microgrid by considering a multi-objective optimization approach. Bilal et al. (Bilal, Nourou, Sambou, Ndiaye, & Ndongo, 2015; Bilal, Sambou, Kébé, Ndiaye, & Ndongo, 2012), the author presented an optimization of stand alone microgrid that minimizes the levelized cost of energy and the CO_2 emission. The results outline that the increasing of levelized cost of energy implies decreasing of CO_2 emission and the photovoltaic modules are more preferred to the wind turbine for hybrid photovoltaic-wind-battery and diesel generator system. An optimal grid-connected to minimize cost of energy and CO_2 emission for residential application using multi-objective genetic algorithm is examined by Abdelshafy et al. (Abdelshafy, Hassan, Mohamed, El-Saady, &

Ookawara, 2017). The microgrid consists of photovoltaic arrays-wind turbine, hydrogen tank, battery, diesel generator, fuel cell, and electrolyzer systems. The results demonstrate exorbitant cost when using battery only or fuel cell as backup energy system. In a research conducted by Lamadica et al. (Lamedica, Santini, Ruvio, Palagi, & Rossetta, 2018), a multi-objective minimizing the operating & maintenance cost of the PV and wind plants and the purchase cost of network energy using Mixed Integer Linear Programming (MILP) proposed. The obtained results show the usefulness of the methodology to identify the optimal parameters which combines the needs of the industrial plant with the renewable energy sources (RES) availability and the achievable savings. Additionally, majority of researches focusing on grid-connected photovoltaic system do not point out multi-objective approach since they explored a single objective which neglect other objectives such as: expected energy not-delivered, total life cycle cost, tilt angle, levelized cost of energy, annualized cost of system, expected excessive energy supplied, greenhouse gases emissions, among others.

2.3 Control methods used

To ensure superior performances in terms of operation and energy efficiency of microgrid photovoltaic energy systems, several optimal operation controls have been developed as per literature. This can be done either in open loop or closed-loop optimal control systems. An open loop optimal operation control presents cost-effectiveness, great stability, and ease to implement, while a closed-loop optimal control mechanism can deal with the uncertainties and disturbances through feedback mechanisms.

From the open loop optimal control systems perspective, many control mechanisms have been used. For example, an optimal operation control of grid-connected photovoltaic-wind turbine-battery under time of use tariff is examined in a study conducted by Phiri et al. (Phiri & Kusakana, 2016). The proposed optimal operation control did not deal with uncertainties and disturbances in photovoltaic power output and electrical load demand. Furthermore, the charging and discharging constraints of battery storage systems was not taken into account in their research. The optimal operation control of microgrid minimizes the power consumption and maximizes the PV-array of grid-connected photovoltaic, diesel generator, and battery system using multiple diesel generators as backup system is discussed by Alramlawi et al. (Alramlawi et al., 2018b). Results prove that the proposed microgrid can supply a continuous power to the load and significantly reduced the total energy cost. The authors did not take into account the reduction of operation cost of diesel generators, various constraints within the microgrid energy system with demand side management program. In a study by Maleki et al. (Maleki, Rosen, & Pourfayaz, 2017), the authors developed an optimal operation of a grid-connected hybrid renewable energy system that consists of photovoltaic, wind turbine, fuel cell, and solar thermal collector for residential applications. The optimal operation control did not take into account the demand response strategies. In another study by Riffoneau et al. (Riffonneau, Bacha, Barruel, & Ploix, 2011), the authors developed an optimal power flow management mechanism for grid-connected photovoltaic system with batteries to assist intensive penetration of photovoltaic production into grid by considering peak shaving. In a research by Kusakana (Kusakana, 2017), the author examined, an energy management of a grid connected photovoltaic-hydrokinetic-battery hybrid system under time of use tariff. The proposed microgrid under the optimal energy management can minimize the operation cost. In a different study by Kusakana (Kusakana, 2016a), the author discussed an optimal operation power flow for grid-connected photovoltaic-battery hybrid system to minimize electricity cost subject to operational constraints. The optimal operation model showed the maximal use of photovoltaic energy and battery energy system.

From the commercial and industrial applications viewpoint, researches have been conducted in terms of open loop optimal control schemes. In a research by Li et al. (H. Li, Eseye, Zhang, & Zheng, 2017), an optimal energy management scheme for economic operation of industrial microgrids under both island and grid-connected modes is examined. In a study by Shi et al. (Shi, Cui, Wen, Guo, & Xue, 2017), the authors present an economic operation model for industrial microgrids with several types of flexible loads such as thermal loads, electric vehicle, and charging loads. However, the microgrid did not consider the diesel generator that is commonly used as backup system in most industrial facilities.

From the closed-loop systems point of view, various closed-loop mechanisms can be used for operation control of microgrid energy systems. The proportional integral derivative (PID) are only suitable for single input single output (SISO) systems and cannot determine the optimal values of the system Hossain, Pota, Issa, and Hossain (2017). The fuzzy logic controller (FLC) presents the drawback in terms of output power oscillations despite its better performance for decision making. On the other hand, the artificial neural network (ANN) has slow dynamic response and sensitivity performances. The H_∞ controllers do not handle constraints such as saturations and they require deep mathematical models (Hossain et al., 2017; Izadbakhsh, Rezvani, & Gandomkar, 2014). In addition, linear quadratic regulator (LQR) and Linear quadratic integrator (LQI) solve the optimization problem within a fixed window while model predictive control (MPC) strategies solve the same problem using a moving horizon which exhibits superior performances (Wang, 2009).

In fact, many control schemes have been proposed for optimal control strategies of microgrid energy system. Similarly, they have also been applied in small scale applications. In a study conducted by Wu et al. (Wu et al., 2015), an open loop and closed-loop optimal operation control are investigated for microgrid-connected photovoltaic-battery system. The objective was to minimize the cost of purchasing electricity from the grid and the wearing cost of the system while maximizing the income of selling power to the grid. It has been demonstrated that the closed-loop on the basis of model predictive control (MPC) presents great control performances in terms of disturbances and accuracy. In a study discussed by Zhang et al. (Zhang, Zhang, Wang, Liu, & Guo, 2015), a model predictive control for grid-connected residential microgrid in order to minimize the operation cost while considering deregulated electricity market and forecast uncertainties was carried out. In another research by Parisio (Parisio, Rikos, & Glielmo, 2014), an optimal operation power dispatch is proposed where a model predictive control with mixed integer linear programming (MILP) is applied. The operation cost is minimized while satisfying a time-varying request and controllable generators minimum operation time and stop time. In this study, the authors did not take into account the reactive power management and sensitivity analysis of the optimization parameters. In a research carried out by Alramlawi et al. (Alramlawi, Gabash, Mohagheghi, & Li, 2018a) an optimal operation control grid connected photovoltaic-battery considering grid scheduled power outage and battery life time using economic model predictive control (EMPC) is examined. It can be observed that the proposed strategy presents a significant reduction of energy cost purchased from the grid while minimizing the curtailment of generated PV-array power and maximizing the battery lifetime. An optimal operation control to minimize the operation cost and losses in microgrid-connected Wind-PV-Battery-Diesel Generator using particle swarm optimization (PSO) and fuzzy logic control (FLC) algorithms is developed in a study discussed by Soontornwuttikrai et al. (Soontornwuttikrai & Raphisak, n.d.). However, the minimization of greenhouse gases emissions for environmental benefits was not taken into account. The optimization operation control of microgrid-connected Wind-PV- Battery- Electric vehicle using artificial neural network (ANN) in order to minimize the power from utility grid and maximize the renewable energy power supplied was investigated by Tamilnesan (Tamilnesan & Vijayanand, 2016). However, the proposed control strategy did not consider the demand response program for the enhancement of the energy efficiency of the microgrid energy system.

Furthermore, most of large scale applications rely on closed-loop systems because of their superior performances which include: robustness, handling of non-linearities and constraints, among others. In a study conducted by Alramlawi et al. (Alramlawi, Mohagheghi, & Li, 2019), a predictive active-reactive optimal power of photovoltaic-battery-diesel microgrid considering the reactive power and battery lifetime costs is investigated. The results showed that proposed economic model predictive control (EMPC) strategy leads to an important reduction of total cost of active and reactive power while at the same time maximizes battery lifetime. However, the authors did not consider minimization of the diesel operation costs and the constraints related to the control variables.

2.4 Mathematical modeling of the grid-connected photovoltaic-diesel generator system

2.4.1 Grid energy

The grid is modelled as an infinite bus capable of either supplying power to the electric loads whenever photovoltaic energy is insufficient or accepting excess photovoltaic energy through a suitable feed-in tariff (K. Ndwali et al., 2020b; S. Sichilalu, Tazvinga, & Xia, 2016; Wanjiru, Sichilalu, & Xia, 2017b). The grid utility provides power to supplement the photovoltaic power in order to meet the load demand and it consumes the excess photovoltaic power (Abbes, Martinez, & Champenois, 2014; K. Ndwali et al., 2020b; Nurunnabi et al., 2019). The grid can be bounded within a certain range which is given by

$$-\infty \leq P_{grid}(t) \leq +\infty, \tag{2.1}$$

here $P_{grid}(t)$ denotes the supplied power from the grid.

The university setup where most of the activities take place between 7:00 hrs and

18:00 hrs is considered. The energy purchased from the main grid between 7:00 hrs and 18:00 hrs is given by

$$E_{grid} = \sum_{t=7}^{18} t_s P_{grid}(t) \tag{2.2}$$

where $P_{grid}(t)$ denotes the grid power, and t_s is the sampling time.
Additionally, the cost of energy (COE) purchased from the main grid 7:00 hrs and 18:00 hrs can be expressed as

$$COE = C_f \sum_{t=7}^{18} t_s P_{grid}(t), \tag{2.3}$$

where $P_{grid}(t)$ denotes the grid power, C_f is the cost of energy per kWh, and t_s is the sampling time [h].

Taking into account power outage of grid utility, active power available can be given by

$$P_{grid}(t) = \alpha_g(t) P_{grid}(t), \tag{2.4}$$

where $\alpha_g(t) \in (0, 1)$ is the grid availability parameter at time t. The power grid is available when $\alpha_g(t) = 1$, and in case of outage power of grid utility $\alpha_g(t) = 0$.

2.4.2 Photovoltaic energy system

Photovoltaic panels produce electricity from solar energy. A solar cell is the fundamental component to transform sunlight into electricity. The connection of many cells constitute a module whereas series-parallel connection of modules constitute a array (Abbes et al., 2014; Belkaid, Colak, & Isik, 2016; Tazvinga, Xia, & Zhang, 2013; Tazvinga, Zhu, & Xia, 2014). The power output of photovoltaic depends on the area of photovoltaic panel, efficiency of photovoltaic, solar radiance, and ambient temperature. The output power of a photovoltaic array is given by

Abbes et al. (Abbes et al., 2014):

$$P_{pv}(t) = \eta_{pv} A_{pv} I(t), \tag{2.5}$$

where A_{pv} denotes the area of photovoltaic array, $I(t)$ denotes the solar irradiation incident on the photovoltaic array at time t, η_{pv} denotes the efficiency of the photovoltaic generator.

The power generated by the photovoltaic plant is given by

$$P_{pv,p}(t) = N_{pv} P_{pv}(t), \tag{2.6}$$

where N_{pv} represents the number of photovoltaic arrays. The simplified solar irradiation which is dependent on the time of the day is given by Wu et al. (Wu et al., 2015)

$$I(t) = R_B\Big(I_B(t) + I_D(t)\Big) + I_D(t), \tag{2.7}$$

where R_B is the geometric factor that represents the ratio of beam irradiation incident on the tilted plane to the standard irradiation on the horizontal plane, $I_B(t)$ is the hourly global irradiation and $I_D(t)$ is the diffuse irradiation.

Photovoltaic efficiency function of hourly insolation and ambient temperature is expressed as given by Abbes et al. (Abbes et al., 2014):

$$\eta_{pv} = \eta_r \eta_{pc}\Big(1 - \beta(T_c - NOCT)\Big), \tag{2.8}$$

where η_r denotes the manufacturer rated efficiency of the module making up the photovoltaic array, η_{pc} is the power conditioning efficiency, β is the generator efficiency temperature factor, ranging from 0.004-0.006 per $^{\circ}C$, T_c cell temperature, and $NOCT$ denotes the normal operating cell temperature. A typical value of

$NOCT$ equals to 45 °C. The cell temperature is expressed as Abbes et al. (2014)

$$T_c = 30 + 0.0175\big(I(t) - 300\big) + 1.14\big(Ta - 25\big), \tag{2.9}$$

where T_a denotes the ambient temperature, while $I(t)$ is the solar irradiation at time t.

Additionally, the limited number of photovoltaic arrays, X_{pv}, is bounded such that,

$$N_{pv}^{min} \leq X_{pv} \leq N_{pv}^{max}, \tag{2.10}$$

where N_{pv}^{min} is taken as zero, while $N_{pv}^{max} = \frac{A_T}{A_{pv}}$. here A_T is the total surface area available at the site, and A_{pv} is the surface area of unit photovoltaic array.

2.4.3 Diesel generator

Diesel generators have commonly been used in the power system, for many decades as one of sources power generation in microgrids (Sufyan, Tan, Abd Rahim, Raihan, & Muhammad, 2018). Generally, they have been utilized as backup system to ensure uninterrupted power supply in order to avoid lost of production in commercial and industrial facilities. The great advantage of using diesel generators as backup system is the fact that it can be operated at any time. However, the diesel generators present high operation & maintenance (O&M) costs and emit greenhouse gases, which are harmful to the environment (Adefarati & Bansal, 2017a; Elmitwally & Rashed, 2010; Goyal & Mehta, 2015). Both non-linear and linear modelling of diesel generator were considered in this research.

2.4.3.1 Nonlinear model of diesel generator system

The fuel consumption of the diesel generator depends on the instantaneous output power and the running time (Alramlawi et al., 2018b). As stated by Adefarati et al. (Adefarati & Bansal, 2017a), the fuel consumption model of diesel generator is developed as a quadratic function and it is modelled according to its parameters as follows;

$$F_{dg}(t) = F_c\Big(aP_{dg}^2(t) + bP_{dg}(t) + c\Big), \tag{2.11}$$

where $P_{dg}(t)$ is the diesel generator power output delivered, F_c denotes the fuel price (\$/L), and the generator coefficients a, b and c are the fuel cost function coefficients of the diesel generators energy systems. They are obtained from the manufacturer's data of diesel generator. In literature, the following coefficients have always been adopted: $a = 0.246$ L/kWh^2 , $b = 0.08145$ L/kWh, and $c = 0.42$ (S. M. Sichilalu & Xia, 2015).

2.4.3.2 Linear model of diesel generator system

The fuel consumption of the diesel generator can also be modelled as a linear function. According to Mohammed et al. (Mohammed, Pasupuleti, Khatib, & Elmenreich, 2015), diesel generator is modelled in conjunction with its parameters where its delivered power is given by;

$$F_{dg}(k) = \begin{cases} F_c\Big(aP_{dg}(k) + b_d P_{ndg}\Big) \text{ if } P_{dg}(k) > 0 \\ 0 \text{ if } P_{dg}(k) = 0 \end{cases}, \tag{2.12}$$

where P_{ndg} represents the nominal power of diesel generator, F_c denotes the fuel price (\$/L), and the generator coefficients a and b_d which are obtained from the manufacturer's data. The following coefficients have always been adopted in literature: $a = 0.246$ L/kWh and $b = 0.08145$ L/kWh Dufo-Lopez and Bernal-Agustín (2008); S. M. Sichilalu and Xia (2015).

As stated by Adefarati et al. (Adefarati & Bansal, 2017b), the power generated P_{dg}

can be estimated in terms of nominal power generated by the diesel generator as;

$$P_{dg} = P_{ndg} \times N_{dg} \times \eta_{dg} \tag{2.13}$$

where N_{dg} is the number of diesel generator and η_{dg} is the efficiency of the diesel generator. Therefore, the Eq. 2.12 can be rewritten as

$$F_{dg}(k) = F_c\Big(aP_{dg}(k) + \frac{b_d P_{dg}(k)}{N_{dg}\eta_{dg}}\Big) \tag{2.14}$$

By denoting τ_{dg} as

$$\tau_{dg} = \frac{b_d}{N_{dg}\eta_{dg}} \tag{2.15}$$

The fuel consumption cost is expressed as

$$F_{dg}(k) = F_c\Big(a + \tau_{dg}\Big)P_{dg}(k) \tag{2.16}$$

2.4.3.3 Capacity of fuel tank

The dynamics of the volume of fuel in the tank can be expressed in the discrete time domain as follows

$$V(k+1) = V(k) - t_s\big(aP_{dg}(k) + \tau_{dg}P_{dg}(k))10^{-3}, \tag{2.17}$$

where, t_s is sampling time and $V(k)$ is the fuel's volume within the diesel generator tank at time k.

The tank should not be completely empty in order to avoid air getting into the fuel injection pump which can cause damage to the pump and injectors (Jarrett, 1995;

Obispo, 2019). Therefore, the amount of fuel in the tank is bounded by the tank dimensions as follows

$$V_{min} \leq V(k) \leq V_{max}, \tag{2.18}$$

Here, V_{min} and V_{max} are the minimum and maximum allowable volumes of the fuel in the tank, respectively. The tank shape is assumed to be cuboid and its maximum volume is expressed as

$$V_{max} = L \times l \times h, \tag{2.19}$$

where L, l and h which are the length, width and height of the diesel tank operated at Engineering workshop JKUAT respectively. It can be deduced that the cross-sectional area A_t is expressed as

$$A_t = L \times l, \tag{2.20}$$

From the feedback point of view, Eq. 2.17 can be modeled in terms of the height of fuel in the diesel tank as;

$$h(k+1) = h(k) - \frac{1}{A_t} t_s \big(aP_{dg}(k) + \tau_{dg} P_{dg}(k)\big) 10^{-3}, \tag{2.21}$$

Where $h(k)$ is the height of fuel in the diesel tank at sampling time k and τ_{dg} denotes a constant parameter of the diesel generator which alters to the second part of Eq. 2.12 to depend on diesel generator power output. Level sensors are cost-effective and are easy to implement in measurement of the tank volume (Wanjiru, Sichilalu, & Xia, 2017a). The Eq. 2.21 can be modelled as

$$h(k+1) = h(o) - \frac{1}{A_t} t_s \big(a + \tau_{dg}\big) 10^{-3} \sum_{j=1}^{k} P_{dg}(j), \tag{2.22}$$

The level of the fuel in the tank must be restricted as

$$h_{min} \leq h(k) \leq h_{max}. \tag{2.23}$$

2.4.4 Inverter model

An inverter is mandatory in a grid- connected photovoltaic system that supplies alternating current (AC) loads because it efficiently transforms the direct current (DC) produced by the photovoltaic power plant to alternating current AC. It is used as a power processing interface between photovoltaic plant and utility grid. Moreover, it provides the synchronization with the utility grid Alhaddad and Alsaad (2016); Bilal et al. (2012). The power output of the inverter is given by

$$P_{inv}(t) = P_{pv}(t)\eta_{inv}, \tag{2.24}$$

where $P_{pv}(t)$ is the photovoltaic power output, and η_{inv} denotes efficiency of inverter. Due to efficient and safe operation, the rating power of inverter should be oversized by between 10% and 30% compared to photovoltaic plant Alhaddad and Alsaad (2016); Ramli, Hiendro, and Twaha (2015). The power rating of an inverter is expressed as

$$Pr_{inv} = P_{pv}(t)X_{pv}K_{inv}, \tag{2.25}$$

where $P_{pv}(t)$ denotes the photovoltaic power, X_{pv} is the number of photovoltaic panels, while K_{inv} denotes oversize coefficient of inverter.

The lifetime of inverter is less than the lifespan of the project and photovoltaic panels. The number of times during lifetime of project that inverter is required to be replaced is expressed by

$$Rep_{inv} = \frac{N}{L_{inv}} - 1, \tag{2.26}$$

where N denotes the lifespan of the project, while L_{inv} denotes the lifespan of inverter.

2.4.5 Demand side management model

As stated in the introduction, the optimal operation control of the microgrid-connected photovoltaic-diesel generator backup system aims at minimizing the operating cost within the framework of demand side management (DSM). The TOU program is the typical demand side management which is considered in this work. The TOU strategy assigns high prices to the peak hours and low prices to the off-peak hours (Harding, Kettler, & Lamarche, 2019; Tan, Yang, & Nehorai, 2014). As noted in (Limited, 2019), The daily electricity price for the Commercial & Industrial 1(CI1) tariff in Kenya which is applied to the selected site is expressed as

$$\rho(t) = \begin{cases} \rho_{off} = & 0.06\$, t \in \text{ 00:00 hrs} - \text{ 6:00 hrs and} \\ & \text{22:00 hrs} - \text{ 00:00 hrs}, \\ \rho_{peak} = & 0.12\$, t \in \text{ 6:00 hrs} - \text{ 22:00 hrs} \end{cases} \tag{2.27}$$

where ρ_{peak} denotes the peak price period and ρ_{off} denotes the off-peak price period.

2.5 Summary of research gaps

In this chapter, the overview of research developments in the area of optimization sizing and optimal operation control applied to microgrid energy systems are outlined alongside their formulated approaches. It has been shown that the randomness of renewable energy sources, the frequent power outage of grid utility, and the variability of load demands make the optimization of microgrid energy system a challenging task. It is evident from the literature review that several researches have been carried out on grid-connected photovoltaic energy system in regard to optimization sizing and optimal operation control strategy for enhancement of reliability, energy efficiency, and resiliency of microgrid. From the sizing perspective, most of studies have focused on a single objective while disregarding other objectives. It has been demonstrated that grid-connected photovoltaic energy systems do not require battery energy storage systems for large scale and industrial applications. Reliability performances of microgrid may be reduced when the storage energy system are left out. Grid connected photovoltaic batteryless systems can be sized in order to improve the reliability with cost-effectiveness. To further improve the performances of microgrid energy systems the optimal operation control is required. It has been pointed out that the optimal operation control along with demand side management program can improve the operation and energy efficiency of microgrid connected energy systems. Finally, the chapter also highlighted some gaps that can be carried out in microgrid sizing and optimal operation control research areas. The following gaps have been identified:

- The cost effectiveness of grid-connected photovoltaic batteryless system for large scale or industrial applications when there is no net-metering within the jurisdiction is not determined.
- The capacity of the battery energy system to the changing of the charging & discharging rate under peurkert's law is not considered for residential applications.
- The leakage and full charge & discharge capabilities in the modelling of battery energy systems is not taken into consideration in small scale applications.
- The consideration of other renewable energy sources such as: waves, tidal, among others; are not included in most microgrid energy systems.
- The consideration of some types of energy storage systems are not included in most microgrid energy systems such as kinetic energy storage (flywheel),

hydrogen storage system, among others.

- Most optimal operation control strategies are not simultaneously taken into consideration the demand side management, demand response, and various constrained in microgrid energy systems.
- High penetration, non-linearity and stochastic nature of renewable energy sources are not considered at the same time in microgrid energy systems.
- Most of researches in the optimization sizing and optimal operation control consider single objective function while disregarding other objective functions. Other objectives include: Grid energy cost, expected energy not-delivered, loss of power supply probability, green house gases emissions, fuel consumption cost, expected excessive energy, battery life time, total life cycle cost, among other objectives.

Dynamic operation control and demand side management program have shown great benefits in microgrid-connected energy system. Since energy storage systems exhibit great economic drawbacks for large scale applications, diesel generator backups have been considered as a cost-effective alternative to enhance the reliability of microgrid (Alramlawi et al., 2018b; Elmitwally & Rashed, 2010). Accordingly, there is necessity of carrying out the optimal operation control in conjunction with the demand side management program for large scale applications such as commercial and industrial facilities to improve the operational and energy efficiency, and resilience of microgrid energy systems. Therefore, the optimal operation control on the basis of an open loop and closed-loop mechanisms of a microgrid-connected photovoltaic-diesel generator backup system under demand side management can be performed. This study addressed the most cost-effective grid-connected photovoltaic batteryless system in order to lower the total life cycle cost and grid energy while maximizing the reliability requirement. This is achieved by considering the optimal operation control by simultaneously minimizes the grid energy cost and fuel consumption cost of diesel generator, while considering the technical and operational constraints.

CHAPTER THREE

MULTI-OBJECTIVE OPTIMAL SIZING OF GRID-CONNECTED PHOTOVOLTAIC BATTERYLESS SYSTEM

3.1 Schematic layout

The proposed grid-connected photovoltaic energy system is composed of utility grid, photovoltaic plant, inverter DC/AC and various Alternating Current (AC) loads as illustrated in Figure 3.1. As photovoltaic plant generates direct current (DC) power, it is connected to the point of common coupling (PCC) through the DC/AC power converter. Utility grid and loads are directly connected to the point of common coupling without any interfacing power conditioning device. The loads can be firstly supplied by photovoltaic solar power P_{pv}, while the utility grid P_{grid} acts as backup to provide load power demand whenever photovoltaic energy is insufficient. The proposed energy system does not necessitate dumping loads because the grid can receive surplus photovoltaic power generated. The grid supplies electricity when power grid is greater than zero ($P_{grid}(t) > 0$). The mathematical models of different components within the grid-connected photovoltaic system are represented as follows

3.2 Economic analysis

Economic evaluation plays an important role in the optimization design of hybrid energy systems. In this research, total life cycle cost (TLCC) is considered as economic index to evaluate the project. Total life cycle cost is an economic

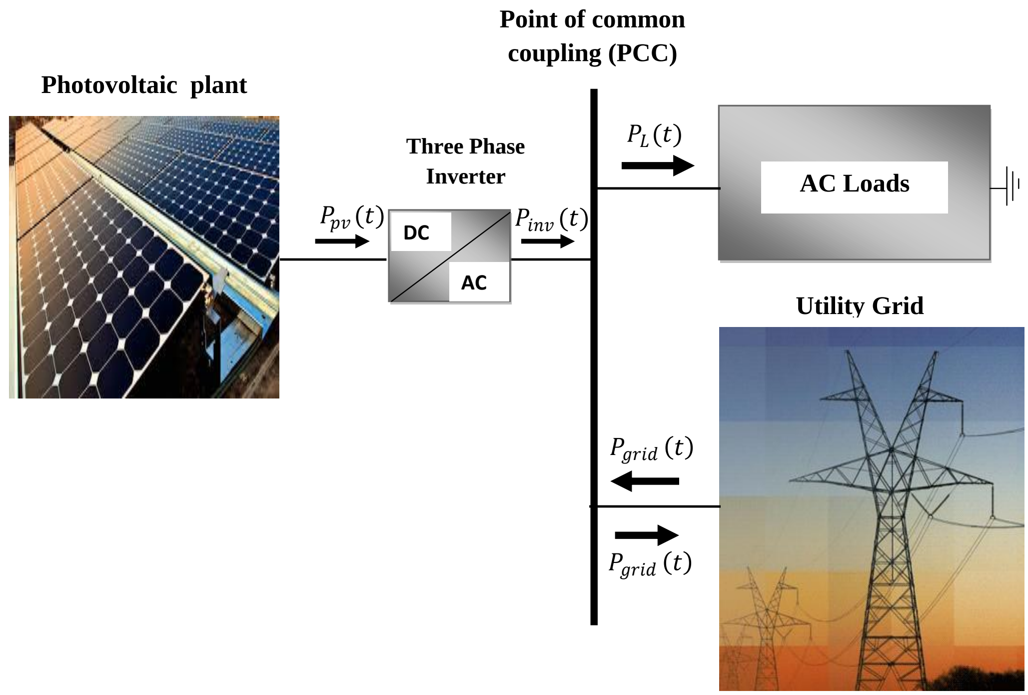

Figure 3.1: Schematic layout of the grid-connected photovoltaic batteryless system

parameter carried out throughout lifespan of the project by considering the cost of all components. Life cycle cost of each component of the grid- connected photovoltaic system is the sum of investment, operation and maintenance cost, replacement cost, minus salvage cost (Abbes et al., 2014). The life cycle cost of each component is given by (**?**)

$$LCC = I_{nvst} + C_{O\&M} + C_{repl} - C_{salv}, \tag{3.1}$$

where I_{nvst} denotes the investment cost, $C_{O\&M}$ denotes the operating and maintenance cost, C_{repl} is the replacement cost, and C_{salv} denotes the salvage cost. Investment cost encompasses the cost of purchasing and installing the system. Salvage cost is the incurred cost at the end of the project lifetime. Photovoltaic operation and maintenance cost is assumed to be 1% of the cost of photovoltaic system (Kamjoo, Maheri, Dizqah, & Putrus, 2016; Wanjiru et al., 2017a), and installation cost is considered 20% of the initial cost (González, Riba, Rius, & Puig, 2015). In this research salvage cost can be neglected because the lifetime of most of components is equal to the lifespan of the project. The present value of operating & maintenance cost is given by (Kamjoo et al., 2016)

$$\begin{cases} O\&M = (O\&M)_0 \times \frac{1+f}{1-f}\left(1 - \left(\frac{1+f}{1+i}\right)^N\right), i \neq f \\ O\&M = (O\&M)_0 \times N, i = f, \end{cases} \tag{3.2}$$

where, f denotes the inflation rate, i denotes interest rate, and N is the lifespan of the project. In Kenya the average inflation rate is 4.65% while the interest rate is 9% of Kenya (2019); Tradingeconomics (2019).

In addition, the total initial investment cost is the sum of each unit price of various components Ogunjuyigbe, Ayodele, and Akinola (2016). The total investment cost is given by

$$I_{invst} = IC_{pv} + IC_{inv}, \tag{3.3}$$

where IC_{pv} denotes the initial cost of photovoltaic, and IC_{inv} denotes the initial cost of inverter. Taking into account 20 % of installation cost, the initial cost of photovoltaic array is given by

$$IC_{pv} = 1.2X_{pv}C_{pv}P_{pv}(t), \tag{3.4}$$

where X_{pv} denotes the total number of photovoltaic panels, C_{pv} denotes capital cost of photovoltaic array per KW, and $P_{pv}(t)$ denotes photovoltaic output power.
The initial cost of inverter is given by

$$IC_{inv} = 1.2Pr_{inv}C_{inv} = 1.2X_{pv}K_{inv}C_{inv}P_{pv}(t), \tag{3.5}$$

where C_{inv} denotes the capital cost of inverter per kW, Pr_{inv} rating power of inverter,

K_{inv} the oversized coefficient of inverter, X_{pv} denotes the number of photovoltaic panels, and $P_{pv}(t)$ denotes photovoltaic power.

The total life cycle cost of the entire system is the sum of LCC of each component, it is given by

$$TLCC = LCC_{pv} + LCC_{inv}, \tag{3.6}$$

where LCC_{pv} denotes the life cycle cost of photovoltaic arrays, and LLC_{inv} denotes the life cycle cost of inverter.
The economic and characteristic parameters of components used to evaluate the total life cycle cost of the entire energy system in this study are illustrated in Table 3.1. The economic data is taken from (Alibaba, 2019). The photovoltaic panel and three phase inverter are the main components which are involved in total life cycle cost.

Table 3.1: Economic parameters of components

Designations	Photovoltaic Panels	3 Phase Inverter
Cost $/kW	281	148
$(O\&M)$ Cost	1%	-
Instal. cost	20%	20%
Repl. cost	0	148
η_r %	17.5 %	98.5%
Lifespan	25 years	15 years

As shown in Table 3.1, the three phase DC/AC inverter presents low O&M cost, thus can be neglected. The replacement cost of photovoltaic panel is zero due to the fact that the photovoltaic lifespan is equal at the lifetime of the project.

3.3 Reliability analysis

The reliability of a distribution power system is geared towards the reduction of frequency or time of interrupted power. This is a great factor to assess system performances. Loss of power supply probability is one of the indexes that is often considered in the evaluation of the reliability of grid-connected photovoltaic power system (Adefarati & Bansal, 2017a; Luna-Rubio, Trejo-Perea, Vargas-Vázquez, & Ríos-Moreno, 2012). Excepted excessive energy supplied, excess of power supply probability, excepted energy not-delivered, among others indexes can be used to measure the reliability of microgrids. In fact, Low of power supply probability (LPSP) has been considered because of minimizing the losses of feeding power to the utility grid.

Generally, loss of power supply probability is a statistical parameter that denotes the deficiency of distributed power system to supply the load demand. The considered site is the university setup where most activities take place from 7:00 hrs to 18:00 hrs. Fortunately, this matches the range of time during which the solar irradiation is available. From the reliability viewpoint, the range of time can then be defined from 7:00 hrs to 18:00 hrs in this study. Assumption is made by neglecting the wired losses within the distribution power system network considered because the available area of installing the photovoltaic panels and the substation are closer to the Engineering workshops. Loss of power supply probability is expressed as (Luna-Rubio et al., 2012);

$$LPSP = \frac{\sum_{t=7}^{18} LPS(t)}{\sum_{t=7}^{18} P_L(t)}, \tag{3.7}$$

where $LPS(t)$ is the loss of power supply at the sampling time t_s, while $P_L(t)$ is the hourly load power demand. Loss of power supply probability is assumed to be between 0 and 1. If the loss of power supply probability equals to 0, it means the load demand is totally covered and if $LPSP$ =1, the load demand is not at all covered by the power supply. The loss of power supply is given by;

$$LPS(t) = P_{inv}(t) + P_{grid}(t) - P_L(t), \tag{3.8}$$

where $P_{inv}(t)$ denotes the power output from the inverter, $P_{grid}(t)$ denotes grid power, and $P_L(t)$ denotes load power demand.

3.4 Methodology description

In order to carry out the multi-objective optimization sizing of grid-connected photovoltaic without energy storage system, the proposed methodology is divided into: multi-objective optimization, objective function and constraints.

3.4.1 Multi-objective optimization

The optimization problem formulated is solved using the MATLAB optimization toolbox which comprises an extensive library of computational algorithms for solving various optimization problems. This optimization under consideration belongs to the category of linear programming minimization problem. As the number of photovoltaic panels must be integer value and the power from the grid utility a continuous value INTLINPROG solver for mixed integer linear programming (MILP) is used.

A mixed integer linear programming is a linear programming (LP) method with the additional restriction that some variables must take integer values. It integrates the branch-and-bound search mechanism, and the cutting plane algorithms through the variation of branch-cut scheme. The technique consists of improving the searching process by systematically enumerating all the candidates solutions and getting rid of evidently impossible solutions (Bénichou et al., 1971; Carrión & Arroyo, 2006; Inc, 2019b; Padberg & Rinaldi, 1991; Testa, Rucco, & Notarstefano, 2017).

To solve multi-objective optimization problems, mixed integer linear programming requires scalarization method. Scalarization method transforms multi-objective functions into single aggregating function using weights (Gunantara, 2018; Mohamed & Koivo, 2010; Penangsang & Sulistijono, 2014). Then, the cost function and constraints can be solved using canonical form as shown by Numbi et al. (Numbi & Xia, 2015).

In summary, the INTLINPROG solver processes the fundamental strategy to solve mixed integer linear programming as follows

1. Restrict the size of the problem by using linear program preprocessing.
2. Determine an initial released linear programming.
3. Execute mixed integer program preprocessing to restrain the linear program relaxing of the mixed-integer problem.
4. Determine cut generation to further consolidate the linear programming relaxing of the mixed integer problem.
5. Retrieve integer-feasible solutions heuristics.
6. Apply the branch-and-bound algorithm to seek the optimal solution.

INTLINPROG function is free to set options for branching rules and solves the problem at any of these enumerated stages.

3.4.2 Objective function

The total life cycle cost of the project and energy purchased from the utility grid are the objective functions which are considered to be minimized. The objective function can be expressed as

$$\min F = \min\left(w \sum_{q=1}^{p} \left(I_{nvst}(q) + C_{O\&M}(q) + C_{repl}(q) - C_{salv}(q) \right) + (1-w) C_f \sum_{t=7}^{18} t_s P_{grid}(t) \right) \tag{3.9}$$

where p is the number of components to be purchased related to the project, I_{nvst} denotes the investment cost, $C_{O\&M}$ denotes the investment cost, C_{repl} denotes the replacement cost, C_{salv} is the salvage cost, C_f is the cost of energy per kWh, t_s is the sampling period, $P_{grid}(t)$ denotes grid power, w denotes the weighing factor selected to point out the relative importance of lowering each term in the objective function. The hourly solar irradiation and hourly power demand data, the sampling period of 1 hour is chosen. Additionally, the tertiary control level is the slowest in microgrid energy systems with the sampling time of 1 hour.

The optimization variables are the number of photovoltaic panels and the hourly grid powers. The number of photovoltaic arrays must be an integer value, while the hourly powers from utility grid are continuous variables. Therefore, taking into account the decision variables, the objective function Eq. 3.9 can be rewritten as

$$\begin{aligned} \min F = \min \Bigg(w \Bigg[C_{pv} \Bigg(1.2 + 0.1 \frac{1+f}{1-f} \Bigg(1 - \Big(\frac{1+f}{1+i} \Big)^{N} \Bigg) \Bigg) \\ +2.2 \eta_{inv} K_{inv} C_{inv} \sum_{t=7}^{18} t_s X_{pv} P_{pv}(t) Pr_{pv} \Bigg] + (1-w) C_f \sum_{t=7}^{18} t_s P_{grid}(t) \Bigg) \end{aligned} \tag{3.10}$$

where C_{pv} denotes the capital cost of photovoltaic arrays per kW, C_{inv} denotes the capital cost of inverter, f denotes the inflation rate, i denotes the interest rate, η_{inv} denotes the efficient of inverter, K_{inv} denotes oversize coefficient of inverter, t_s the sampling period, X_{pv} denotes the number of photovoltaic arrays, and Pr_{pv} denotes the power rated of photovoltaic, N is the lifespan of the project, w is the weighting factor, C_f is the cost of energy per kWh, $P_{grid}(t)$ denotes power grid. The first term of the objective function represents the total life cycle cost of the project, and second term represents energy purchased from the grid.

3.4.3 Constraints

The entire grid-connected photovoltaic system is subject to some operational and technical constraints between power generations and load demand. In order to maximize the reliability, the LPSP(t) is given by

$$\begin{cases} LPSP \geq 0 \\ \sum_{t=7}^{18} X_{pv} P_{inv}(t) + P_{grid}(t) - P_L(t) \geq 0 \\ \sum_{t=7}^{18} X_{pv} P_{inv}(t) + P_{grid}(t) \geq \sum_{t=7}^{18} P_L(t) \\ -\left(\sum_{t=7}^{18} X_{pv} P_{inv}(t) + P_{grid}(t) \right) \leq -\sum_{t=7}^{18} P_L(t) \end{cases} \tag{3.11}$$

The objective function and constraints are solved using the canonical form in (Numbi & Xia, 2015), such that

$$\min f^T X \tag{3.12}$$

subject to

$$\begin{cases} AX \leq b \\ L_b \leq X \leq U_b \\ X = [X_{pv}, \sum_{t=7}^{18} P_{grid}(t)]^T \\ X_{pv} \in \mathbf{N} \\ P_{grid}(t) \in \mathbf{R} \end{cases} \tag{3.13}$$

The $f^T X$ denotes the objective function to be minimized, X consists of the decision variables that is a vector representing the optimal number of photovoltaic panels and the energy purchased from the grid, A denotes matrix associated with inequality constraints, and b is the scalar related to inequality constraint; L_b is the lower bound vector, and U_b is the upper bound vector of the decision variables.
From Eq. 3.10, it can be assessed that;

$$\left[C_{pv} \left(1.2 + 0.1 \frac{1+f}{1-f} \left(1 - \left(\frac{1+f}{1+i} \right)^N \right) \right) + 2.2 \eta_{inv} K_{inv} C_{inv} \sum_{t=7}^{18} t_s X_{pv} P_{pv}(t) Pr_{pv} \right] = 541.3277 \tag{3.14}$$

The objective function f^T is therefore expressed as

$$f^T = [541.3277w, (1-w) t_s C_f] \tag{3.15}$$

The vector X consists of all the decision variables, it is expressed as

$$X = \left[X_{pv}, \sum_{t=7}^{18} P_{grid}(t) \right]^T \tag{3.16}$$

From the reliability constraint measured by the loss of power supply probability Eq. 3.11, inequality constraint AX in Eq. 3.13 is expressed as

$$AX = \sum_{t=7}^{18} -X_{pv} P_{inv}(t) - P_{grid}(t) \tag{3.17}$$

where $P_{inv}(t)$ is the output power of inverter at time t, $P_{grid}(t)$ is the power supplied by the utility grid. From Eq. 3.16 and Eq. 3.17 the matrix A is given by

$$A = \left[\sum_{t=7}^{18} -P_{inv}(t), -1 \right] \tag{3.18}$$

The scalar b is given by

$$b = \sum_{t=7}^{18} -P_L(t) \tag{3.19}$$

As defined in section 2.1.1 and section 2.1.2, the lower (L_B) and upper (U_B) bounds of the decision variables given in canonical form are expressed as

$$L_B = [0, 0] \tag{3.20}$$

$$U_B = [459, +\infty] \tag{3.21}$$

3.5 Case study and data collection

The setup is the university workshops where most activities happen from 7:00 hrs to 18:00 hrs. The facility consists of various workshops such as: machine tools, carpentry, Ipic, foundry, welding, plumbing, and fitting workshops. Each workshop has various three and single phase types of electrical loads. The data was experimentally collected in the Engineering workshops from October 2018 to April 2019 using three phase power logger Fluke 1735. Figure 3.3 displays the power logger fluke 1735. Its sampling time was set up to 1 minute and the hourly peak power has been selected. The logging has been done for several days during the peak period of consumption. It can be observed from the dynamic variation of the power load demand that during night hours from 19:00 the power consumption is low. It starts increasing at 8:00 in the morning. From the daily load profile, it is shown that the peak load is 64.26 kW between 10:00 hrs and 11:00 hrs and the total daily energy consumption is 1090.5 kWh/day while daytime energy demand of 700.3510 kWh can be deduced. Figure 3.2 shows daily power consumption of Engineering workshops.

The daily power consumption corresponds to the operation of several type of

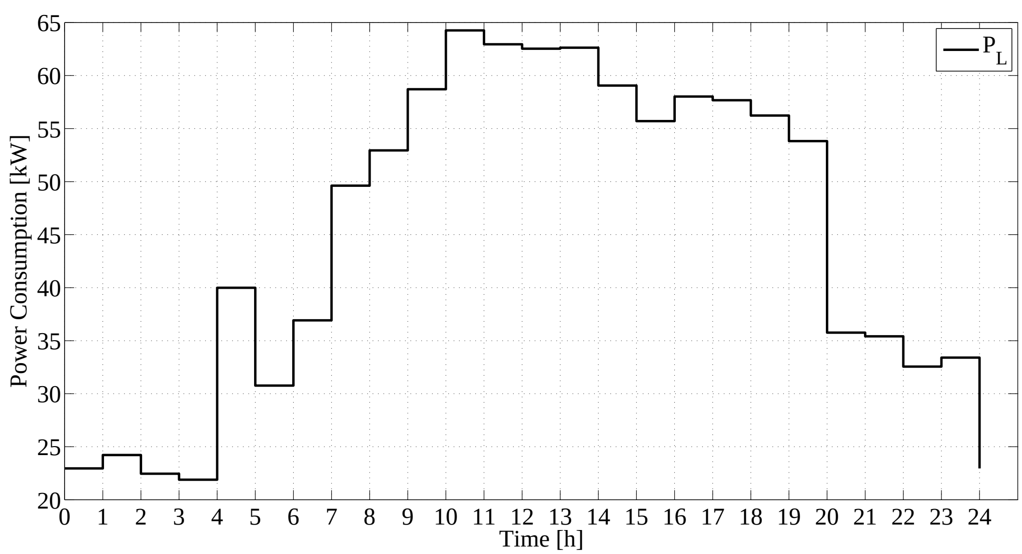

Figure 3.2: Daily power demand of Engineering workshops at JKUAT

equipments such as machine tools, welding machines, and others. The daily load profile is mainly represented by a suite of power demand. The power demand is taken as constant over each time-step of 1 hour. Systematically, the sampling period is 1 hour as illustrated in Figure 3.2.

Figure 3.3: Power Logger Fluke 1735

The selected daytime is from 7:00 hrs to 18:00 hrs when the solar irradiation is available at the site. The workshops power system supply is currently provided by the national grid and diesel generator as backup system. A diesel generator of 250 kVA is used for uninterrupted power supply whenever there is outage of power from main grid. Due to high levelized cost of energy of diesel generator, the assumption is made by considering the availability of the national grid over 24 hours. Thus, the grid utility will be the unique source to feed the load demand when solar radiation is not available. The hourly solar radiance and ambient temperature data of the site are obtained from (Viola, 2019). The optimal sizing of the grid-connected photovoltaic system is derived from a selected day of the most unfavorable month in terms of irradiation. In Kenya, July is considered as the worst month due to the fact the monthly average irradiation is the lowest in comparison with other months. July average irradiation is 4.4 kWh/m^2/day (Tukiainen, 2019). Figure 3.4 shows the average monthly solar irradiation of solar irradiation in Kenya. Additionally, the hourly solar irradiation and the ambient temperature data of the site are obtained from European Commission (Viola, 2019). Figure 3.5 depicts the solar irradiation of the selected day.

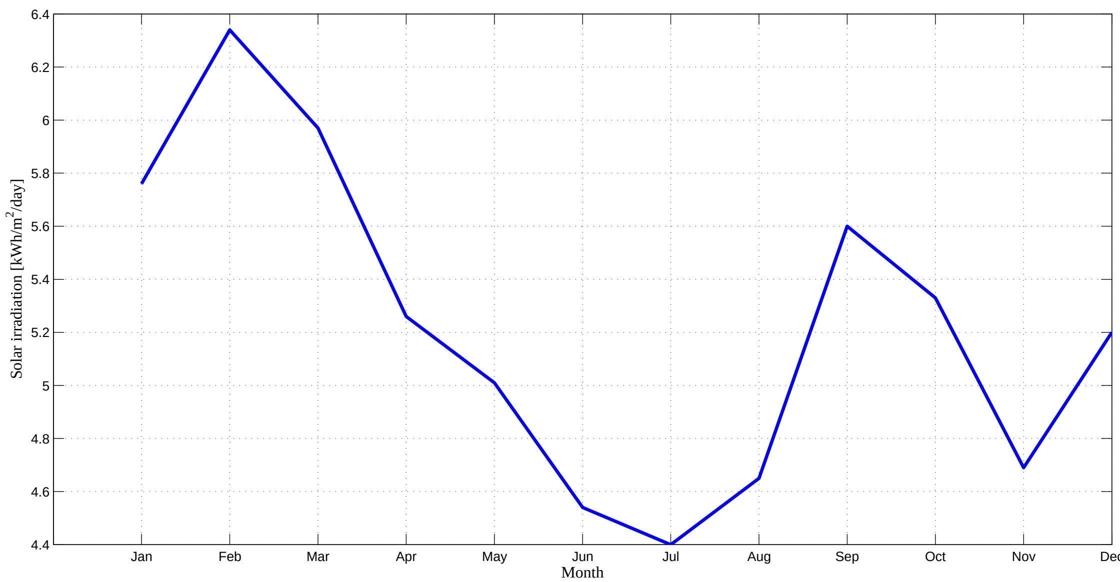

Figure 3.4: Monthly solar irradiation in Kenya

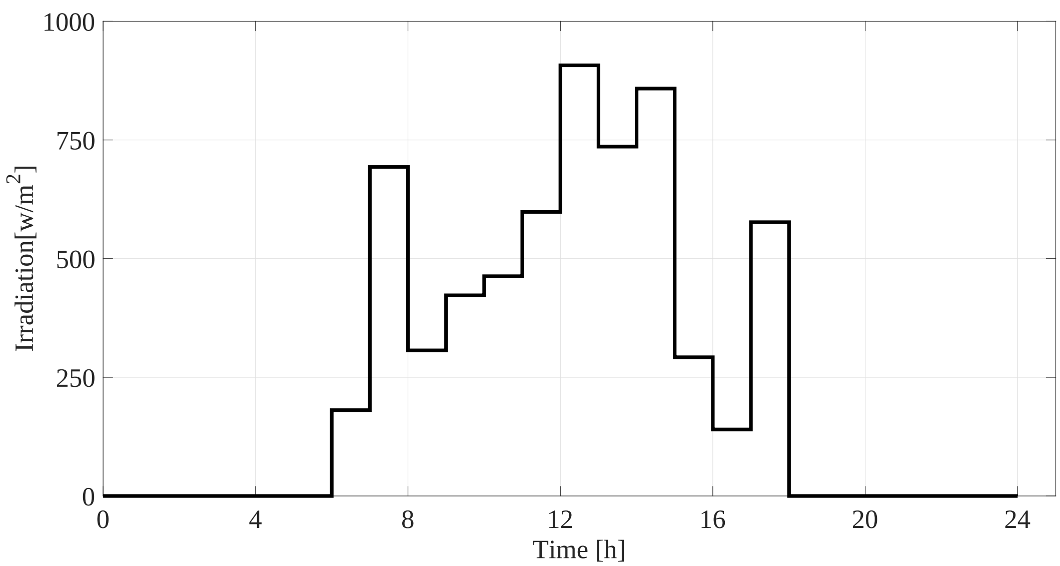

Figure 3.5: Solar irradiation of the selected day

Apart from economic parameters displayed in section 3.2, Table 3.2 shows other different constant parameters used in this study.

Table 3.2: Parameters used in the study (Alibaba, 2019; of Kenya, 2019; Tradingeconomics, 2019)

Parameters	Designations	Values
Project lifetime	N	25 years
Lifetime of PV		25 years
Rated power of PV	P_r	340 W
Rated Efficiency of PV	η_r	17.5%
Area of PV	A_{pv}	1.96 m^2
Available Area	A_T	900 m^2
Inverter lifetime	L_{inv}	15 years
Inverter Efficiency	η_{inv}	98.5%
Inverter factor	K_{inv}	1.25
Sampling time	t_s	1 h
Average inflation rate	f	4.65%
Interest rate	i	9%
weighing factor	w	0.5
Lower bound	L_B	[0 0]
Upper bound	U_b	[459 $+\infty$]
Cost of energy	C_f	0.12 $/kWh

3.6 Results and discussion

This section presents the results obtained for multi-objective optimization sizing of grid connected photovoltaic system without a battery. The baseline of Engineering workshop is the national grid with diesel generator backup system. An assumption is made by considering the availability of grid utility over 24 hours. Hence, from the sizing perspective, the baseline is simply the utility grid in this study which come from literature review and data collection.

The results discussed are related to the grid connected photovoltaic system without the diesel generator due to its high levelized cost of energy. The objective function has been solved using INTLINPROG solver for mixed integer linear programming problem as discussed in section 3.5.1. The photovoltaic power plant has been designed in order to supply the load demand during the daytime hours from 7:00 hrs to 18:00 hrs while maximizing the reliability requirements. Due to the unavailability of radiance solar for the remaining times, grid utility will supply the loads power demand at those specific times.

As JKUAT does not have a power purchase agreement (PPA) with Kenya power lighting company (KPLC), the entire energy system has been designed such that the losses that would arise by feeding power to the grid are minimized. Table 3.3 displays the values of decision variables and total life cycle cost of project when the weighting factor is equal to 0.5.

Table 3.3: Simulation results obtained

Parameters	Designation	Values
Number of PV panels	X_{pv}	354
Energy purchased	E_{grid}	0.6022 kWh
Total life cycle cost	$TLCC$	$191630
Daily energy saving		64.16%
Revenue		$574596.25

The same results in Table 3.3 arise also when a value within the range of $0.376 \leq w \leq 0.664$ is assigned to the weighing factor. It can be deduced that the optimal number of photovoltaic panels is 354, the optimal energy from the grid in daytime is 0.6022 kWh, while the total life cycle cost is found to be 191630$. With this energy system, the grid energy during the daytime between 7:00 hrs and 18:00 hrs has considerably been lowered from 700.3510 kWh to 0.6022 kWh.

The daily energy to supply the loads demand of the Engineering workshop is approximately 1090.5 kWh. Considering the baseline and the cost of electricity 0.12 $/kWh in Kenya (Limited, 2019), the daily energy purchased from the grid cost $ 117.2. The total energy generated by the photovoltaic panels is 699.749 kWh. The economical benefit includes saving of 83.97$ per day in comparison with the baseline considered in this study. The entire energy system can yield a daily energy saving up to 64.16 %.

Varying the weighting factor between $0 \leq w \leq 0.375$ the photovoltaic power plant is prioritized as apposed to the grid utility. The photovoltaic power plant system is oversized so that the optimal energy of the grid utility starts becoming negative. This means that the grid utility absorbs more electrical energy from the photovoltaic power plant. As stated, there is no need to oversize the photovoltaic plant because the facility does not have power purchased agreement with Kenya power and lighting company. This can bring losses that occur by feeding the excess photovoltaic energy to the utility grid. On the other hand, by assigning the weighting factor between $0.665 \leq w \leq 1$ all the power that feeds the loads comes from the grid utility. The INTLINPROG solver has selected the lower bound of the number of photovoltaic panels which is zero as defined. This means the grid is more prioritized to cover the loads demand in the sizing process than the photovoltaic plant.

Besides, the total life cycle cost of the project has been estimated for 25 years, photovoltaic energy generated during this lifetime of the project can be evaluated to be 776226.25\$. Therefore, the savings which can be generated from installing the photovoltaic energy system connected to the grid is approximately 574596.25\$. This shows that the grid connected photovoltaic batteryless system can clearly be profitable to end-user customer at demand side in this region for the chosen facility.

3.7 Summary

In this chapter, the development of a novel optimization methodology on the basis of multi-objective optimal sizing of grid-connected photovoltaic without energy storage systems is carried out. The optimization design seeks to minimize the total life cycle cost and energy purchased from the grid while at the same time satisfying the reliability constraint. In fact, the reliability is measured by the loss of power supply probability index. Mixed integer linear programming is used to find the optimal values of decision variables, namely the number of photovoltaic panels and energy purchased from the utility grid. This model considerably lowers the daily electricity cost by reducing the energy purchased during daytime which is much beneficial at customer side. This approach ensures efficient and reliable grid-connected photovoltaic system and can be suitable for any application wherever energy storage systems may present exorbitant cost. From the optimization results obtained, the optimal sizing consists of 354 photovoltaic panels, the energy purchased from the grid during the daytime is 0.6022 kWh, and the total life cycle cost of the project is estimated $ 191630. With these optimal values, the proposed power supply cover the load demand during daytime hours from 7:00 hrs to 18:00 hrs while guaranteeing the reliability requirement. Grid utility can be the main power source to supply load demand only during the remaining times. The daily energy saving is up to 64.16% in comparison with the baseline, and the economical benefit for the lifetime of the project arises to $574596.25. Varying the weighing factor affects the multi-objective optimization sizing of grid- connected photovoltaic batteryless energy system accordingly. The optimal weighting factor can be taken between 0.376 and 0.664 for most cost-effective grid-connected photovoltaic batteryless system. The theory and results discussed in this chapter have been published as journal paper K. Ndwali et al. (2020b).

CHAPTER FOUR

OPTIMAL OPERATION CONTROL OF MICROGRID-CONNECTED UNDER TIME OF USE TARIFF

4.1 Schematic layout

The proposed microgrid consists of utility grid, photovoltaic plant, diesel generator, and various loads as shown in Figure 4.1. All the generated power sources and loads are connected to the point of common coupling (PCC). The priority is to feed the loads with photovoltaic solar energy, while the utility grid and diesel generator act as backup energy systems. In other words, if the load demand is greater than photovoltaic power, the deficit power is covered by the main grid utility. However, in case of power outage from utility grid, diesel generator provides the electricity. On the other hand, if the photovoltaic power is greater than power load demand, the excess is fed to the grid utility.

4.2 Optimization problem

4.2.1 Objective function

The model-based optimization control that uses advanced control mechanism is designed in this chapter. The optimal operation control seeks to simultaneously minimize the energy purchased from utility grid and the fuel consumption cost of diesel driven generator. To this sense, the aim of optimal operation control is to economically and efficiently distribute the hourly power generated with maximum

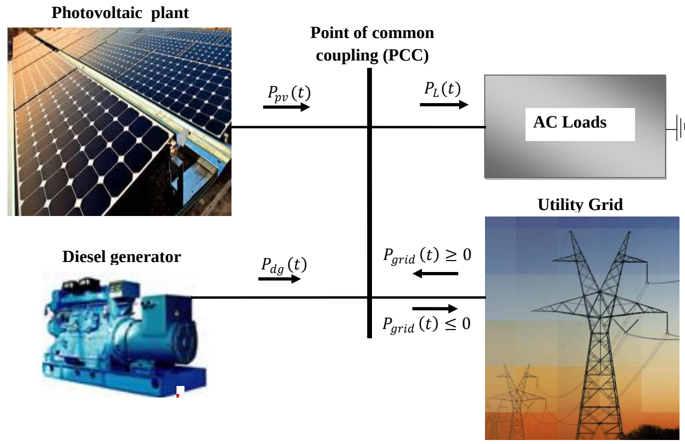

Figure 4.1: Schematic layout of the grid-connected photovoltaic with diesel backup

benefit. The objective function is given by

$$\min F = \min\left(\omega t_s \sum_{t=1}^{N} \rho(t) P_{grid}(t) + (1-\omega) F_c t_s \sum_{t=1}^{N} \left(a P_{dg}^2(t) + b P_{dg}(t) + c\right)\right), \quad (4.1)$$

where $\rho(t)$ denotes the cost of energy, F_c denotes the fuel cost, t_s is the sampling time, $P_{grid}(t)$ denotes grid utility power, $P_{pv}(t)$ is the photovoltaic power, $P_{dg}(t)$ represents diesel generator power output, N is the range of time horizon, ω denotes the weighting factor. The diesel generator factors a, b, and c are obtained for the manufacturer's data as outlined in chapter 2.

In the objective function represented by Eq. 4.1, the first term aims at minimizing energy purchased from the grid, while the second term minimizes the fuel consumption cost of the conventional diesel generator. The variables are the hourly grid power and diesel generator power outputs.

4.2.2 Constraints

The proposed microgrid-connected energy system contains linear and non-linear constraints. The non-linear constraints are caused by the quadratic function of fuel consumption diesel generator and the fact that power grid and diesel generator power output cannot operate simultaneously to supply power to the loads. Mathematically, the entire system is subject to the following technical, and operational constraints. The hourly power balance for meeting the load demand is expressed as;

$$P_L(t) = P_{grid}(t) + P_{pv}(t) + P_{dg}(t), \tag{4.2}$$

where $P_{grid}(t)$ denotes the grid power, $P_{pv}(t)$ is the photovoltaic power, and $P_{dg}(t)$ represents diesel generator power at instant t.

Moreover, the total photovoltaic power generation can be used to cater for the loads and the surplus is fed into the utility grid. Photovoltaic power is bounded as;

$$0 \leq P_{pv}(t) \leq P_{pv}^{max}(t), \tag{4.3}$$

where $P_{pv}^{max}(t)$ denotes maximum photovoltaic power output at time t.
Due to high levelized cost of diesel generator power in comparison with grid utility, both of them cannot supply power at the same time. The diesel generator acts as backup to ensure uninterrupted power supply in case of grid power outage. The open loop controller should be capable of considering the constraint related to grid utility and diesel generator operation cost in commercial and industrial facilities in Kenya. Putting into account this economic factor regarding levelized cost of energy, this restriction introduces the equality non-linearity constraint which is expressed as;

$$P_{grid}(t) \times P_{dg}(t) = 0, \tag{4.4}$$

The power output limits of diesel generator is restricted by the following bounds,

$$0 \leq P_{dg}(t) \leq P_{dg}^{rated}, \tag{4.5}$$

where P_{dg}^{rated} denotes the rated power of the diesel generator.

The grid can feed the loads or receive power from photovoltaic solar energy. The utility grid is bounded by;

$$-\infty \leq P_{grid}(t) \leq +\infty, \tag{4.6}$$

where $P_{grid}(t)$ is the power grid at instant t.

4.2.3 Open loop control algorithm

The grid power and diesel generator power are the controllable variables. Due to non-linearity of the diesel generator, FMINCON in MATLAB is the suitable solver selected to carry out the formulated optimization problem. The objective function and constraints are solved using the canonical form (Messac, 2015) presented by

$$\min_{X} \Big(f(X) \Big) \tag{4.7}$$

subject to

$$\begin{cases} A_{eq}X = b_{eq}, \\ L_b \leq X \leq U_b. \end{cases} \tag{4.8}$$

Here, $f(X)$ represents the objective function to be minimized which contains linear and non-linear functions. The vector X consists of all control variables in the optimization problem, A_{eq} and b_{eq} are coefficients associated with linear equality constraints, while L_b and U_b are lower and upper bounds of variables. The non-linear equality constraint Eq. 4.4 is modelled by assigning the grid availability parameter

α either by 1 or 0.

The objective function $f(X)$ is given by

$$f(X) = \left(\omega \sum_{1}^{N} \rho(1:N)'.*X(1:N)+(1-\omega)F_c \sum_{N+1}^{2N} \left(aX^2(N+1:2N)+bX(N+1:2N)+c\right)\right) \tag{4.9}$$

The control variable vector X is expressed as

$$X = \Big[P_{grid}(1), \quad ... \quad P_{grid}(N), \quad P_{dg}(1), \quad ... \quad P_{dg}(N)\Big]^{T}_{1\times 2N}, \tag{4.10}$$

From the power balance equality constraint Eq. 4.2, matrix A_{eq} is expressed as

$$A_{eq} = \left.\begin{bmatrix} 1 & 0 & \cdots & 0 & |1 & 0 & \cdots & 0 \\ 0 & 1 & \cdots & 0 & |0 & 1 & \cdots & 0 \\ \vdots & \vdots & \ddots & \vdots & |\vdots & \vdots & \ddots & \vdots \\ 0 & 0 & \cdots & 1 & |0 & 0 & \cdots & 1 \end{bmatrix}_{N\times 2N} \right| \tag{4.11}$$

The vector b_{eq} is given by

$$b_{eq} = \Big[P_L(1) \quad \cdots \quad P_L(N)\Big] - \Big[P_{pv}(1) \quad \cdots \quad P_{pv}(N)\Big]^{T}_{1\times N} \tag{4.12}$$

where $P_L(N)$ is the hourly power consumption and $P_{pv}(N)$ is the hourly photovoltaic power.

The limits of control variables are between the lower (L_b), and upper bounds (U_b) such that

$$L_b = \Big[-\infty \quad \cdots \quad -\infty_N, \quad 0 \quad \cdots \quad 0_N\Big]^{T}_{1\times 2N} \text{ and} \tag{4.13}$$

$$U_b = \Big[+\infty \quad \cdots \quad +\infty_N, P_{dg}^{rated} \quad \cdots \quad P_{dg,N}^{rated}\Big]^{T}_{1\times 2N} \tag{4.14}$$

4.2.3.1 Optimization solver and algorithm

The linear and non-linearity problems can be solved through discretization which is the process of transforming continuous models and equations into discrete counterparts. The discretization process is usually performed as the first step toward making them suitable for numerical assessment and implementation on digital computers (Lustgarten, Gopalakrishnan, Grover, & Visweswaran, 2008; Sakamoto, Hori, & Ochi, 2011). The problem formulated above belongs to the class of constrained non-linear multivariable optimization. It can therefore be solved using nonlinear solvers. Additionally, Matlab optimization toolbox contains an extensive library of computational algorithms for solving various optimization problems. In Matlab, multidimensional constrained non-linear minimization problems can be suitably solved using FMINCON solver. The FMINCON solver uses a Hessian as the optional input and it is the second derivatives of the Lagrangian. Various FMINCON algorithms handle Hessian inputs differently such as interior point, active set, sequential quadratic programming, among other algorithms (Agnarsson, Sunde, & Ermilova, 2013; Coleman, Branch, & Grace, 1999; Messac, 2015). Hessian inputs are the inputs of second derivative functions of the objective function. Figure 4.2 shows the flow chart of FMINCON solver interior point algorithm (Messac, 2015).

Where X_0, A_{eq}, b_{eq}, U_B and L_B are the input variables which must be defined. The variable X_{opt} is the optimal vector of variables. The interior point algorithm FMINCON solver is chosen because of its ability to solve large scale optimization problems and is known to converge faster than other types of algorithms (Inc, 2019c; Messac, 2015).

To analyze the effectiveness of the proposed open loop algorithm, a real case study presented in section 3.6 is considered. The rated power of a photovoltaic panel is 340 w as stated in chapter 3. Table 4.1 depicts various constant parameters used in this chapter for simulation.

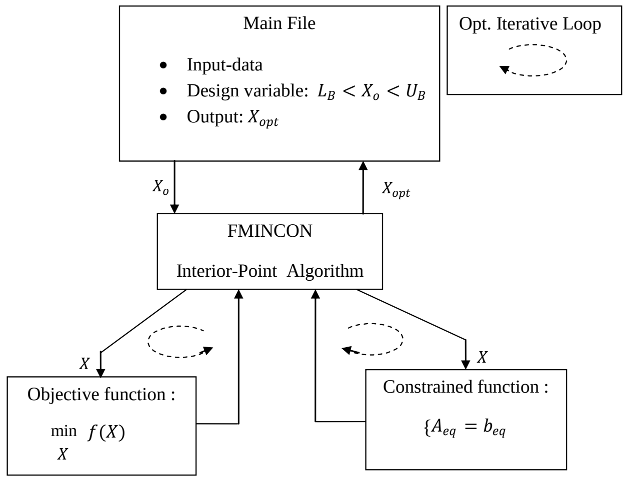

Figure 4.2: Flow chart of Fmincon solver interior-point algorithmMessac (2015)

Table 4.1: Parameters used for simulationAlibaba (2019); K. Ndwali et al. (2020b); of Kenya (2019); Tradingeconomics (2019)

Parameters	Designations	Values
Cost of energy	C_f	0.06\$/kWh
		0.12 \$/kWh
Feed in tariff	F_d	0.12\$/kWh
Fuel cost	F_c	0.973 \$/L
Rated power of a photovoltaic panel	P_r	340 W
Number of photovoltaic panels	N_{pv}	354
Rated power of diesel generator	S_{dg}	250 kVA
Power factor of diesel generator	Cosϕ	0.8
Diesel parameter	a	0.246
Diesel parameter	b	0.08145
Diesel parameter	c	0.42
Sampling time	t_s	1 hr
Time horizon	N	24

4.3 Results and discussion

This section presents simulation results of using open loop controller to optimally and efficiently operate the grid- connected photovoltaic with diesel backup system under demand side management program. This is a constrained non-linear multi-variables optimization problem solved using FMINCON interior-point algorithm. As a baseline of the facility the utility grid supplies the instantaneous loads power demand and diesel generator acts as backup. The simulation is carried out to demonstrate the minimization of daily operational cost of microgrid under the intermittent mode (IM) and intermittent connected mode (ICM). The sampling time t_s is 1 hour and the time horizon 24 hours. In this work, two scenarios were considered. In case I, the intermittent mode is considered when the grid power outage has been taking place between 7:00 hrs and 18:00 hrs. The grid power outage is indicated by assigning the grid availability parameter $\alpha(t) = 0$ at that specific period of time. On the other hand, the intermittent connected mode has been considered as case II. It mainly represents the case where the grid utility is available over 24 hours. This is carried out by attributing the grid availability parameter $\alpha(t) = 1$, over 24 hours time horizon. The simulation of both cases, intermittent mode and intermittent connected mode is done by assigning different values of the weighting factors, ω. Since it is assumed that there is neither energy storage system nor dumping loads; hence, whenever the photovoltaic energy is surplus, it is sold to the utility grid through an appropriate feed-in tariff.

Case I

The important difference between the two operational scenarios is that in case I, the optimal operation control operates by considering electricity outage between 7:00 hrs and 18:00 hrs. Since the facility is in the university setup, this illustrates the worst period when the electricity outage occurs between 7:00 hrs and 18:00 hrs. It is evident that the baseline, defined as the diesel generator can operate in case of electricity outage and the grid utility supplies power in the absence of photovoltaic power from 18:00 hrs to 7:00 hrs. In this scenario, the grid availability parameter is set $\alpha(t) = 0$ between 7:00 hrs and 18:00 hrs, altering some upper bound grid power elements to 0 for that specific period of electricity outage. Figure 4.3 depicts the optimal operation control strategy without considering the incorporation of photovoltaic plant system as presented in (K. Ndwali et al., 2020b). The objective function considered minimizes the fuel consumption cost Eq. 2.11. This is conducted by considering the price of diesel generator of \$ 0.973 as noted in **?**. The above

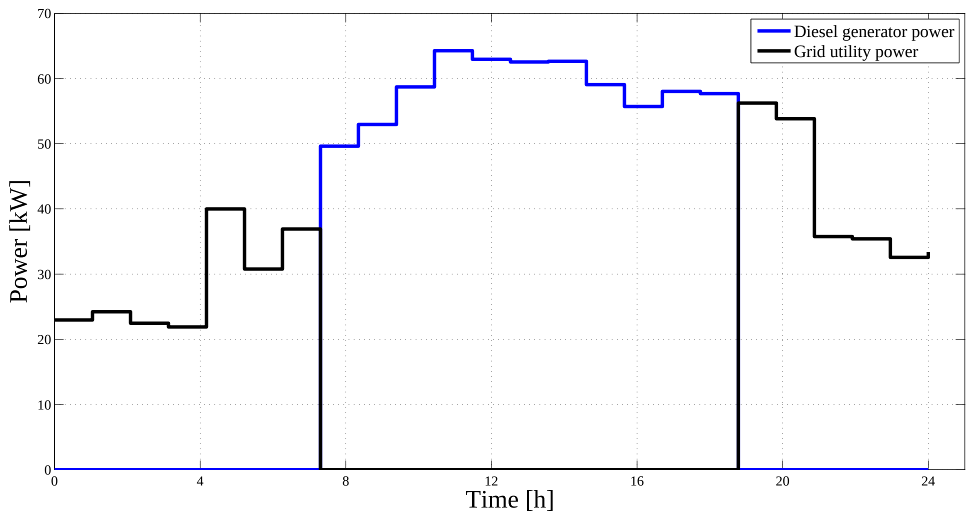

Figure 4.3: Microgrid-diesel generator backup power flow in intermittent mode

scenario presents the benefit of considering the open loop control strategy without photovoltaic plant system. Table 4.2 shows various parameters related to energy and cost in this scenario obtained from figure 4.3. This scenario in intermittent mode

Table 4.2: Optimal operation control without considering the photovoltaic plant system

Parameters	Value
Baseline (Grid & Diesel generator)	1090.5kWh
Diesel generator without optimal controller	700.3510kWh
Diesel generator with optimal controller	644.2kWh
Optimal grid energy	446.3kWh
Cost of Grid + Diesel generator	\$ 574.4

can be advanced by taking into account the photovoltaic plant system as optimally designed by Ndwali et al. (K. Ndwali et al., 2020b). Figure 4.4 illustrates different optimal power flows over 24 hours within the microgrid connected photovoltaic with diesel generator under intermittent mode. In fact, this figure presents the prevailing optimal result obtained when the weighting factor $\omega = 0.1$. The photovoltaic power feed-in takes place during the daytime as depicted in Figure 4.4.

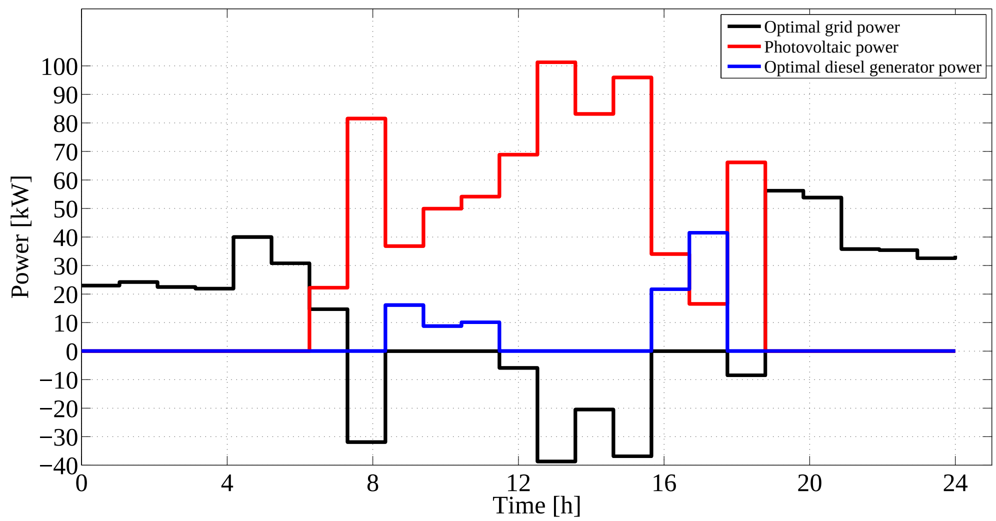

Figure 4.4: Microgrid-connected photovoltaic-diesel generator backup power flow in intermittent mode

The diesel generator provides various output power to supplement the photovoltaic power during the daytime as shown in Figure 4.4. The diesel generator can be operated to supplement the photovoltaic power deficiency, in lieu of covering the load demand from 7:00 hrs to 18:00 hrs as depicted in Figure 4.3. It is operated only 5 hours during daytime, between 8:00 hrs and 11:00 hrs, at last between 15:00 hrs and 17:00 hrs. This infers that the operating cost of diesel generator is considerably reduced. As a result, fuel consumption cost is minimized as well as the greenhouse gases emissions.

In addition, the photovoltaic energy feed-in is found by making the balance between the hourly power demand and the hourly optimal photovoltaic power output. In this scenario, the negative part exhibits the various magnitude powers feed back during the daytime. Table 4.3 displays the baseline, daily optimal energy of diesel generator, grid utility as well as the energy sold from the use of optimal control with photovoltaic solar energy under grid electricity outage in intermittent mode (IM). The optimal diesel energy is the total daily energy delivered by diesel generator,

Table 4.3: Baseline and optimal control in intermittent mode

Parameters	Values
Baseline (Grid & Diesel generator)	1090.5kWh
Optimal diesel generator energy with PV plant	98.2 kWh
Optimal grid energy	424.1 kWh
Diesel Energy not delivered	546 kWh
Energy sold	142.4 kWh
Diesel energy saving	84.8%
Daily Income	$17
Total cost of grid utility + DG	$ 140
Total cost saving	66.6%

while the optimal grid energy is the total daily energy delivered by the grid utility. Further, the energy sold is the daily excess of photovoltaic energy. It is evaluated by subtracting the hourly power consumption and the hourly photovoltaic power output. From the results depicted in Table 4.3, the grid energy and the diesel generator are considerably reduced compared to the baseline. Additionally, the excess photovoltaic energy is sold to the grid utility. By comparing the optimal control strategy of microgrid in intermittent mode considering the photovoltaic plant, the cost of grid and diesel generator saving is up to 20%.

Different results can be obtained by varying the weighting factor in the objective function Eq. 4.1. Table 4.4 shows various figures related to grid energy and diesel generator energy by assigning different values to the weighting factor ω. In general, by varying the weighting factor in the objective function from $\omega = 0$ to $\omega = 1$, the grid energy is gradually reducing while the diesel generator energy is increasing. The diesel generator reaches its lower daily energy value at $\omega = 0.1$. Setting the weighting factor $\omega = 1$, the grid energy reaches its lower daily energy while the diesel generator reaches its maximum daily energy delivered. The cost function related to

Table 4.4: Optimal control with the photovoltaic system

Weighting factor	Grid energy kwh	Diesel generator Energy kWh
0	424.1	98.9
0.1	424.1	98.2
0.2	424	98.9
0.3	424	98.4
0.4	423.9	98.7
0.5	423.6	99.45
0.6	422.8	100.97
0.7	420.4	104.9
0.8	416.65	110.8
0.9	405.1	130
1	-12.5	1950

the grid utility is prioritized in lieu of diesel generator. The diesel generator supplies power to the load demand when the solar irradiation is not available. The grid energy is negative which means that it generally receives more energy. It is evident that this case presents the worst simulation scenario due to the high operating cost of diesel generator. This can be avoided by opening the switch related to the grid utility in order to operate the microgrid autonomously.

Case II

Firstly, intermittent grid connected mode can be evaluated with taking into account the constraint Eq. 4.4. Figure 4.5 shows the optimal power flow output of the microgrid energy system in this scenario. As shown in Figure 4.5, the diesel generator is not operated over 24 hours time horizon when the grid power is available. Varying ω, the results obtained do not change because the formulated operation optimal control aims at only minimizing the grid energy. It is clear that the greenhouse gases emissions are not emitted. Due to the fact that the photovoltaic power is not among control variables, its feed-in graph has been kept unchanged in both intermittent mode and intermittent connected mode. The daily energy and cost saving obtained

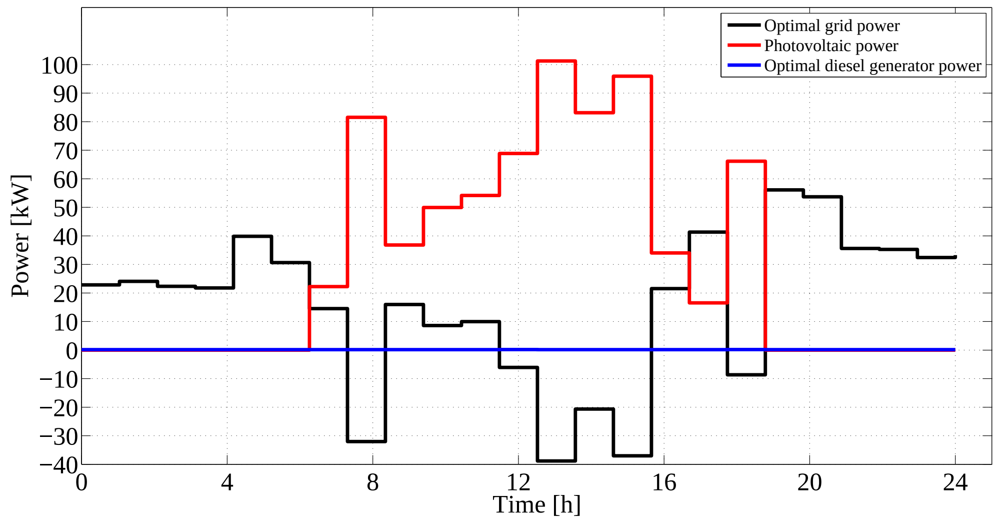

Figure 4.5: Microgrid-connected photovoltaic-diesel generator optimal operation power flow in intermittent connected mode

from the optimal operation control with photovoltaic solar energy are depicted in Table 4.5. The photovoltaic power feed-in takes place between 7:00 hrs and 8:00 hrs, between 11:00 hrs and 15:00 hrs, and between 17:00 hrs and 18:00 hrs with various output powers. The baseline cost is the bill that is paid in the case study before the optimal control scheme. This bill is from the grid utility energy consumed by the loads. If the load demand is only supplied by the grid, the daily electricity represents the baseline cost. The daily income is derived from the energy sold to the grid. The energy sold to the grid is found by respectively subtracting the load demand and the photovoltaic energy energy at each time t. The baseline cost and income are found by considering the cost of electricity and the feed in tariff in Kenya for Commercial & Industrial 1 (CI1) customer is equivalent to 0.12\$/kWh for peak hours and 0.06\$/kWh for off-peak hours (Limited, 2019). Figure 4.5 depicts different optimal power flows over 24 hours time horizon of grid connected photovoltaic with diesel generator backup system when the utility grid is available. The baseline is the current situation where the grid supplies power to the loads because of high levelized cost of energy of diesel generator. The grid utility is prioritized against the diesel generator from the simulation viewpoint. Table 4.5 displays various values related to intermittent connected mode while considering the constraint Eq. 4.4.

Table 4.5: Baseline and optimal control in intermittent connected mode

Parameters	Values
Baseline	1090.5 kWh
Grid energy	522.3 kWh
Energy saving	568.2 kWh
Energy sold	142.4 kWh
Baseline cost	$117.2
Daily Income	$17
Cost saving	58.2%
Energy saving	52.1%

The energy saved indicates the grid power not delivered to the loads that would have been supplied without optimal control. It is thus, the balance between grid power without optimal control and grid power by considering optimal control strategy. The daily revenue generated is obtained by considering the energy sold and the feed in tariff 0.12$/kWh as noted in (Boampong & Phillips, 2016). It can be deduced that the considered microgrid with the use optimal controller yields significant energy saving due to a substantial benefit from photovoltaic plant. From the results obtained, it implies that this microgrid connected photovoltaic-diesel generator backup energy system has a potential of being a cost effective system and beneficial.

Secondly, the intermittent connected mode can be simulated without considering Eq. 4.4. In this scenario, the weighting factor $\omega = 0.1$ is the prevailing simulation which provides the reduction of the use of diesel generator. In daytime, the photovoltaic power plant is the main power supplier to cover the load demand. The power from the grid utility supplements the photovoltaic power whenever it cannot cover the loads. The excess power of photovoltaic plant is fed back to the grid utility at some specific time during daytime. It can be seen that photovoltaic solar constitutes the major contribution of the power supply. During daytime from 7:00 hrs to 18:00 hrs, photovoltaic power supplies the load and the surplus power can be sold to the grid.

However, the grid utility fully supplies the loads from 19:00 hrs to 6:00 hrs in the absence of photovoltaic power output.

Varying the weighting factor ω, the daily energy purchased from the grid and the diesel generator energy vary as well. Table 4.6 presents various results obtained by assigning the weighting factor ω from 0 to 1. As shown in Table 4.6 by increasing

Table 4.6: Optimal operation control in intermittent connected mode

Weighting factor ω	Grid energy purchased kWh	Diesel Generator energy kWh
0	519.89	3.2
0.1	519.6	3.6
0.2	519.2	4.2
0.3	518.6	4.9
0.4	517.5	7
0.5	517.5	7.96
0.6	514.9	10.4
0.7	515	11
0.8	506.5	23
0.9	467.4	96.76
1	-268.6	1615.7

the weighting factor from 0 to 1, the daily grid energy is decreasing while the daily diesel energy is increasing. When the weighting factor $\omega = 1$, the grid energy reaches its lower daily energy while the diesel generator reaches its maximum daily energy delivered. In this regards, the diesel generator supplies power demand and the grid utility receives more energy. Thereby, when the weighting factor $\omega = 1$, the microgrid connected photovoltaic system with diesel generator as backup will present a high operating cost. This exhibits the worst scenario in intermittent connected mode when not taking into account the Eq. 4.4. Therefore, when the diesel generator is prioritized, the microgrid must operate in islanded mode by considering the Eq. 4.4. Compared to the studies conducted by Li et al (H. Li et al., 2017), Alramlawi et al. (Alramlawi et al., 2018b), and Shi et al. (Shi et al., 2017), the proposed method is cost-effective because of considering the demand side management program, minimizing the cost of grid energy and fuel consumption cost. The innovative and efficient optimization algorithm takes also into account the non-linearity of the diesel generator system and the constraints related to levelized cost of energy of distributed energy resources.

4.4 Summary

A novel optimal operation control of microgrid connected photovoltaic-diesel generator system subject to constraints between the controllable variables under demand side management program for commercial and industrial applications in Kenya is developed. More specifically, the time of use is the type of demand side management which is considered in this work. The Engineering workshops at Jomo Kenyatta University of Agriculture and Technology are considered as a case study. The operational control strategy is on the basis of the open loop optimal control over 24 hours time horizon. The FMINCON interior-point algorithm was used to determine the suitable control variables to lower the objective function which seeks to reduce the grid energy cost and the fuel consumption cost of the diesel generator. Generally, open loop control is chosen due to its cost effectiveness and stability. Two scenarios have been considered. On one hand, the intermittent mode is considered, whereby grid outage is between 7:00 hrs and 18:00 hrs, and on the other hand, the intermittent connected mode is considered. From the results obtained, it has been shown that, the optimal operation control under demand side management is remarkable in terms of sustainable and efficient use of electric energy. The benefits of this energy system are significant because it leads to the energy and cost savings as well as generate substantial revenue. This control model is effectively suitable for commercial and industrial facilities in Kenya. The theory and results discussed in this chapter have already been presented in the journal article (P. K. Ndwali, Njiri, & Wanjiru, 2020). This research can be advanced to deal with uncertainties and disturbances which are always present in microgrid systems. Additionally, for more sustainability requirement for step closer to zero-energy buildings, renewable energy sources such as wind turbine, biomass, and hydrogen energy system can be incorporated within the microgrid system.

CHAPTER FIVE

ECONOMIC MODEL PREDICTIVE CONTROL OF MICROGRID-CONNECTED PHOTOVOLTAIC-DIESEL GENERATOR SYSTEM

5.1 Schematic layout

Considering the economic model predictive control (EMPC) strategy, the schematic of the proposed microgrid-connected photovoltaic-diesel generator is shown in Figure 4.1.

5.2 Optimization problem

5.2.1 Objective function

The constrained optimization problem that considers advanced control system is designed. Systematically, the optimal operation control simultaneously searches to minimize the power purchased from utility grid and the fuel consumption cost of diesel driven generator. The objective function is defined in terms of both present and future variables; hence, the objective function at each sampling time k is expressed as;

$$\min F = \min\left(\omega t_s \sum_{j=k}^{k+N_c-1} \rho(j) P_{grid}(j|k) + (1-\omega) F_c t_s (a+\tau_{dg}) \sum_{j=k}^{k+N_c-1} P_{dg}(j|k)\right), \quad (5.1)$$

where $\rho(t)$ denotes the cost of energy, F_c is the fuel cost, $P_{grid}(j/k)$ and $P_{dg}(j/k)$ are grid power and diesel generator power respectively, at j^{th} sampling interval on the basis of the measurement at instant k. Additionally, N_c is the control horizon, ω weighting factor and t_s is the sampling time. The sum of all weighting factors should be equal to 1. The factors a and b are the fuel cost function coefficients of the diesel generator and are obtained for the manufacturer's data as proposed in section 2. In the objective function represented in Eq. 5.1, the first term minimizes the power purchased from the grid, and the second term minimizes the fuel consumption of diesel generator.

5.2.2 Constraints

The considered microgrid- connected energy system is modelled as a constrained linear programming (LP) multi-criteria optimization problem. Mathematically, the entire system is subject to technical constraints such as power generation sources and operational constraints such as demand supply balance, bus voltage limit, and power generation limits. Considering the prediction time horizon, the power supply and the load demand balance within the microgrid is given by

$$P_L(j) = P_{grid}(j|k) + P_{pv}(j) + P_{dg}(j|k), j = k, ...k + Nc - 1, \tag{5.2}$$

where $P_{grid}(j|k)$ and $P_{dg}(j|k)$ represent the predicted grid power and diesel generator power respectively, at j^{th} sampling interval on the basis of information measured at instant k, while $P_{pv}(j)$ is the photovoltaic power. The total photovoltaic power generation can be used to cater for the loads and the surplus is fed into the utility grid. Due to high levelized cost of diesel generator power in comparison with grid utility, both of them cannot supply power at the same time. The diesel generator acts as backup to ensure an uninterrupted power supply in case of grid power outage. Putting into consideration the economic factor regarding levelized cost of energy, this restriction introduces the constraint between the controllable variables inputs. This is implemented by varying the lower bounds of the grid utility accordingly.

The power output limit of diesel generator is restricted such that

$$0 \leq P_{dg}(j|k) \leq P_{ndg}. \tag{5.3}$$

The grid can feed the loads or receive energy when photovoltaic solar energy is excessive. Therefore, the utility grid is bound as follows

$$-\infty \leq P_{grid}(j|k) \leq +\infty, \tag{5.4}$$

5.2.3 Model predictive control algorithm

Closed-loop model predictive control technique allows explicitly handling of optimality and system constraints for multi-variable problems over a finite control horizon. The model predictive control (MPC) scheme is a powerful control strategy applicable to on-line complex optimization problems (Karg & Lucia, 2018). It has the ability to predict the future events, take control action accordingly, and predict the change in the dependent variables caused by independent variables. Moreover, it uses the current plant measurement, dynamic state, the process variable target to calculate the future events. This controller uses predefined cost function to calculate the optimal values of the future control inputs (Badal, Das, Sarker, & Das, 2019; Camponogara, Jia, Krogh, & Talukdar, 2002). The constraints of the system are modelled with respect to its practical limitations and are expressed in a compact form as illustrated in section 2. Figure 5.1 depicts the structure of optimal control on the basis of model predictive control approach (Kaya & Attia, 2007). Generally, the plant model stands for the system to be controlled as shown in Figure 5.1. The output of the plant is either measured through sensors or estimated through kalman filter (KF) or observer. In particular, the optimization strategy processes the optimal control sequences by minimizing a defined objective function subject to some constraints. The dynamic optimizer simply represents the selected solver for

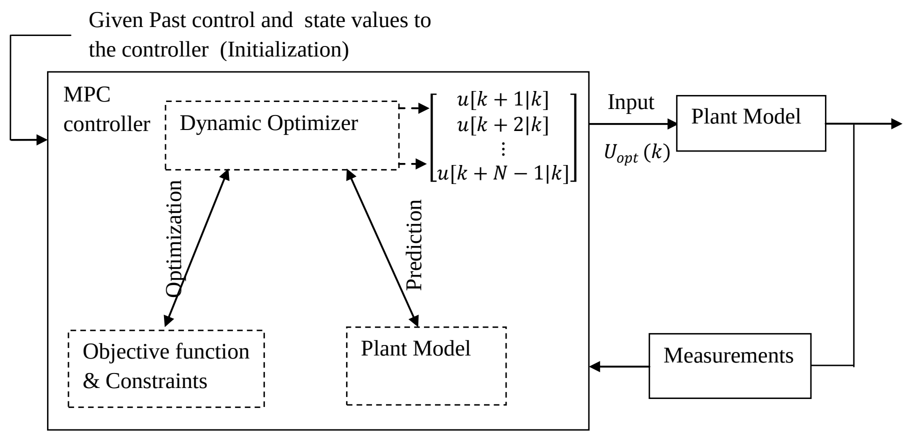

Figure 5.1: Structure of optimal control based on model predictive control approach

optimization at each sampling time. The MPC scheme requires that only the first optimal control of each input is applied at each sampling time.

In the process of designing the optimal control based on MPC, the daily power demand and the photovoltaic power output are forecasted. However, the hourly power demand and the photovoltaic power can deviate from the forecasted values within microgrid systems. Such deviations are considered as system disturbances on both the power demand and photovoltaic power. Solving this optimal operation control, linear state space control is deduced from the microgrid- connected photovoltaic-diesel generator backup system. Similar to the open loop algorithm, the control vector X which contains all the control variables is expressed as;

$$X(k) = [P_{grid}(k|k) \cdots P_{grid}(k + Nc - 1|k), P_{dg}(k|k) \cdots P_{dg}(k + Nc - 1|k)]. \quad (5.5)$$

The controller determines the time k, and it calculates the control horizon N_c. Afterwards, it solves an open loop optimization problem with the operating horizon N_c to obtain an optimal solution, where only the first element of the control variables

P_{grid} and P_{dg} are implemented into the microgrid. From the control standpoint, microgrid-connected photovoltaic-diesel generator system is modelled as Multi-Input Multi-Output (MIMO) system. The main advantage of the model predictive control over other control strategies is the ability to optimize multi-variable, while dealing with constraints, as well as forecast possible future behaviors of the system (Wang, 2009). Model predictive control optimization problem includes both control N_c and predicting horizon N_p. The control horizon is given by

$$N_c = N - k + 1, \tag{5.6}$$

where N is the total number of samples in the operating horizon of 24h.
Model predictive control approach solves the optimization problem as follows (Wanjiru et al., 2017a)

1. Determine the control horizon $N_c(k)$ using Eq. 5.6 for each sampling time k,
2. Determine the optimum solution within the control horizon;
    - Minimize the cost function Eq. 5.1;
    - Subject to constraints;
3. Execute the first switching control to the microgrid energy system $[P_{grid}(1|k), P_{dg}(1|k)]$ from the optimum solution;
4. Measure the state variable which is the level of fuel inside the diesel tank;
5. Set $k = k + 1$, and update system states, inputs, and output;
6. Repeat step 1-5 until k reaches a predefined value.

This optimization problem is solved using linear programming (LP) in OPTI Toolbox which is a free Matlab Toolbox for solving linear optimization problem. The linear programming can be solved in an easy, fast, and reliable manner Messac (2015).

5.2.4 Mathematical model formulation

The objective function and constraints are solved using the canonical form as proposed in (P. K. Ndwali et al., 2020; Tazvinga et al., 2014; Wanjiru et al., 2017b) and are given by ;

$$\begin{cases} f^T X \\ A_{eq} X = b_{eq} \\ AX \leq b \\ L_b \leq X \leq U_b. \end{cases} \tag{5.7}$$

The $f^T X$ is the linear objective function to be minimized and vector X consists of all control variables in the optimization problem. The A_{eq} and b_{eq} are coefficients associated with equality constraints, while L_b and U_b are lower and upper bounds of variables.

From the Eq. 5.1 the canonical form $f^T X$ is expressed as

$$f^T = [\omega t_s \rho(j) \cdots \omega t_s \rho(N), (1-\omega) t_s (a + \tau_{dg}) F_c(j) \cdots (1-\omega) t_s (a + \tau_{dg}) F_c(N)]_{1 \times 2N_c}. \tag{5.8}$$

The vector X consists of all controllable variables and it is given by

$$X = [P_{grid}(j) \cdots P_{grid}(N), P_{dg}(j) \cdots P_{dg}(N)]_{1 \times 2N_c}. \tag{5.9}$$

From the power balance equality constraint in Eq. 5.2, matrix A_{eq} is expressed as

$$A_{eq} = \left. \begin{bmatrix} 1 & 0 & \cdots & 0 & |1 & 0 & \cdots & 0 & | \\ 0 & 1 & \cdots & 0 & |0 & 1 & \cdots & 0 & | \\ \vdots & \vdots & \ddots & \vdots & |\vdots & \vdots & \ddots & \vdots & | \\ 0 & 0 & \cdots & 1 & |0 & 0 & \cdots & 1 & | \end{bmatrix}_{N_c \times 2N_c} \right|. \tag{5.10}$$

The vector b_{eq} is given by

$$b_{eq} = \begin{bmatrix} P_L(j) & \cdots & P_L(N_c) \end{bmatrix}^T_{1\times N_c} - \begin{bmatrix} P_{pv}(j) & \cdots & P_{pv}(N_c) \end{bmatrix}^T_{1\times N_c}. \tag{5.11}$$

Similarly, the inequality constraints can be derived from the Eq. 2.23.

$$\begin{cases} h_{min} \leq h(k) \Rightarrow -h(k) \leq -h_{min} \\ h(k) \leq h_{max} \end{cases} \tag{5.12}$$

From the Eq. 5.12, the inequality constraints is transformed to

$$\begin{cases} A_1 X \leq b_1 \\ A_2 X \leq b_2 \end{cases} \tag{5.13}$$

$$A_1 = \frac{t_s(a+\tau_{dg})10^{-3}}{A_t} \left. \begin{bmatrix} 0 & 0 & \cdots & 0 & |1 & 0 & \cdots & 0 & | \\ 0 & 0 & \cdots & 0 & |1 & 1 & \cdots & 0 & | \\ \vdots & \vdots & \ddots & \vdots & |\vdots & \vdots & \ddots & \vdots & | \\ 0 & 0 & \cdots & 0 & |1 & 1 & \cdots & 1 & | \end{bmatrix}_{N_c\times 2N_c} \right|, \tag{5.14}$$

$$A_2 = -\frac{t_s(a+\tau_{dg})10^{-3}}{A_t} \left. \begin{bmatrix} 0 & 0 & \cdots & 0 & |1 & 0 & \cdots & 0 & | \\ 0 & 0 & \cdots & 0 & |1 & 1 & \cdots & 0 & | \\ \vdots & \vdots & \ddots & \vdots & |\vdots & \vdots & \ddots & \vdots & | \\ 0 & 0 & \cdots & 0 & |1 & 1 & \cdots & 1 & | \end{bmatrix}_{N_c\times 2N_c} \right|, \tag{5.15}$$

$$b_1 = \begin{bmatrix} h(o) - h_{min} & \cdots & h(o) - h_{min} \end{bmatrix}^T_{1\times N_c}, \tag{5.16}$$

and

$$b_2 = \begin{bmatrix} h_{max} - h(o) & \cdots & h_{max} - h(o) \end{bmatrix}^T_{1\times N_c}. \tag{5.17}$$

The linear inequality in canonical form in Eq. 5.7 is expressed as

$$\begin{bmatrix} A1 \\ A2 \end{bmatrix} X \leq \begin{bmatrix} b1 \\ b2 \end{bmatrix}. \tag{5.18}$$

The limits of control variables are between the lower (L_b) and upper bounds (U_b). When there is no PV plant system, the lower bound of the grid utility is zero to avoid the diesel generator power to be sold to the grid utility. However, when considering the PV plant system the lower bound is $-\infty$ in order to enable the excess photovoltaic power to be sold to the grid utility. This condition is implemented in the EMPC algorithm by using an if-else loop. The lower (L_b) and upper bounds (U_b) are therefore expressed as

$$L_b = \begin{bmatrix} 0 & \cdots & 0_{Nc}, & 0 & \cdots & 0_{Nc} \end{bmatrix}^T_{1\times 2N_c}, \tag{5.19}$$

$$L_b = \begin{bmatrix} -\infty & \cdots & -\infty_{Nc}, & 0 & \cdots & 0_{Nc} \end{bmatrix}^T_{1\times 2N_c}, \tag{5.20}$$

and

$$U_b = \begin{bmatrix} +\infty & \cdots & +\infty_{Nc}, & P_{ndg} & \cdots & P_{ndg,Nc} \end{bmatrix}^T_{1\times 2N_c}. \tag{5.21}$$

Additionally, Table 5.1 shows various constant parameters used for simulation in this chapter in order to analyze the effectiveness of the EMPC strategy.

5.3 Results and discussion

Two cases were investigated based on the EMPC scheme of microgrid connected photovoltaic-diesel generator system. The first case was carried out by considering the intermittent mode when the grid outage occurs between 7:00 hrs and 18:00 hrs when most university activities take place. The second case is carried out in the intermittent connected mode when grid power availability is considered over 24 hours time horizon.

Table 5.1: Parameters used in simulation (Alibaba, 2019; K. Ndwali et al., 2020b; of Kenya, 2019; Tradingeconomics, 2019)

Parameters	Designations	Values
Cost of energy	$\rho(t)$	0.06\$/kWh
		0.12 \$/kWh
Feed in tariff	F_d	0.12\$/kWh
Fuel cost	F_c	0.973 \$/L
Number of photovoltaic panels	N_{pv}	354
Number of diesel generator	N_{dg}	1
Rated power of diesel generator		250 kVA
Nominal active power of diesel generator	P_{ndg}	200 kW
Power factor of diesel generator	$\cos\phi$	0.8
Efficiency of diesel generator	η_{dg}	35%
Diesel parameter	a	0.246
Diesel parameter	b_d	0.08145
Length of DG tank	L	1.48m
Width of DG tank	l	1.02 m
height of DG tank	h_{max}	0.23 m
Minimal level of the fuel in the DG tank	h_{min}	0.005 m
Initial level of the fuel in the DG tank	h_o	0.225 m
Sampling time	t_s	1 h
Time horizon	N	24

Case I

The proposed model predictive control is used to operate the microgrid in intermittent mode considering the worst scenario where grid power outage happens between 7:00 hrs and 18:00 hrs. This can be analyzed by designing the economic model predictive control by not considering the impact of photovoltaic plant system. On the other hand, the performances of EMPC is analyzed by considering the optimization sizing of photovoltaic plant as presented in (K. Ndwali et al., 2020b). In this scenario, the baseline constitutes of grid utility and diesel generator which acts as backup energy system. Figure 4.3 shows different power flows without considering the photovoltaic plant system. As displayed in Figure 4.3, the grid utility provides power from 00:00 hours to 7:00 hours and from 18:00 hours to 00:00 hrs while the conventional diesel generator supplies the loads when power outage occurs from 7:00

hours to 18:00 hours. Table 4.2 depicts various results obtained in intermittent mode without considering the photovoltaic plant system. The baseline cost represents the daily invoice that is paid before the incorporation of photovoltaic plant system in intermittent mode. Although, the diesel generator supplies power in peak price period, this presents the most expensive normal scenario. This is because of the negative factor of the diesel generator, namely high levelized cost of energy. The EMPC cannot provide any saving in the intermittent mode because it only have the diesel generator as one source of power during the daytime. The EMPC takes into consideration the constraints related to the fuel level in the diesel tank and the dynamics of fuel is presented in Figure 5.2. The level of fuel has substantially

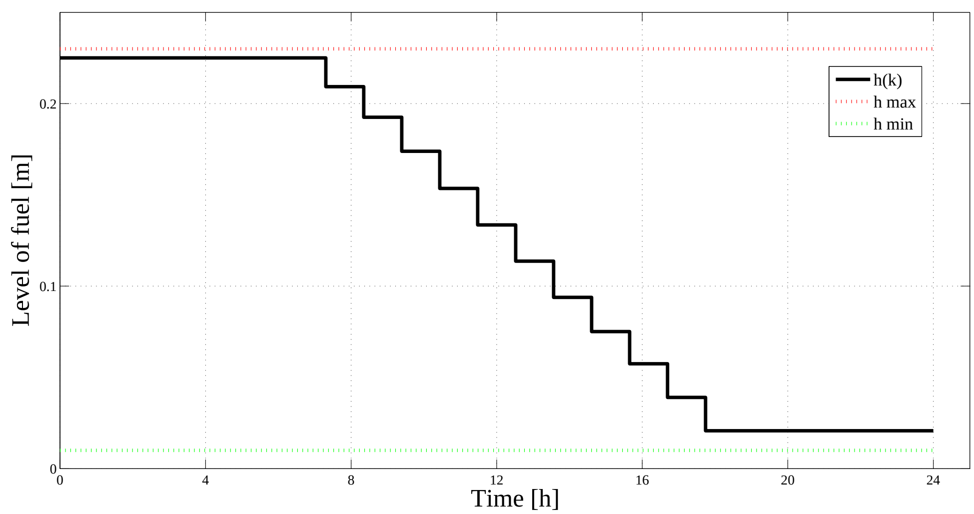

Figure 5.2: level of fuel in intermittent mode without photovoltaic plant system

decreased in the diesel tank in IM without considering the PV plant system. Setting the weighting factor between $0 \leq \omega \leq 1$ by considering the restriction between grid utility and diesel generator system, various performances of EMPC can be observed. Table 5.2 shows different performances in respect to total grid energy and diesel energy in this scenario. When the weighting factor lies between $0.619 \leq \omega \leq 1$, the diesel generator energy is increased by covering the load demand in the evening

Table 5.2: Model predictive control in intermittent mode without photovoltaic plant system

Weighting factor ω	Grid energy kWh	Diesel generator kWh
0 - 0.618	446.36	644.1
0.619-1	380.96	709.53

hours from 18:00 hours to 22:00 hours despite the grid availability at that specific period of time. The grid utility supplies the load demand at 23 hours. Figure 5.3 displays the power flows output within the microgrid when the weighting factor is between $0.619 \leq \omega \leq 1$. This presents high operational cost because of the use

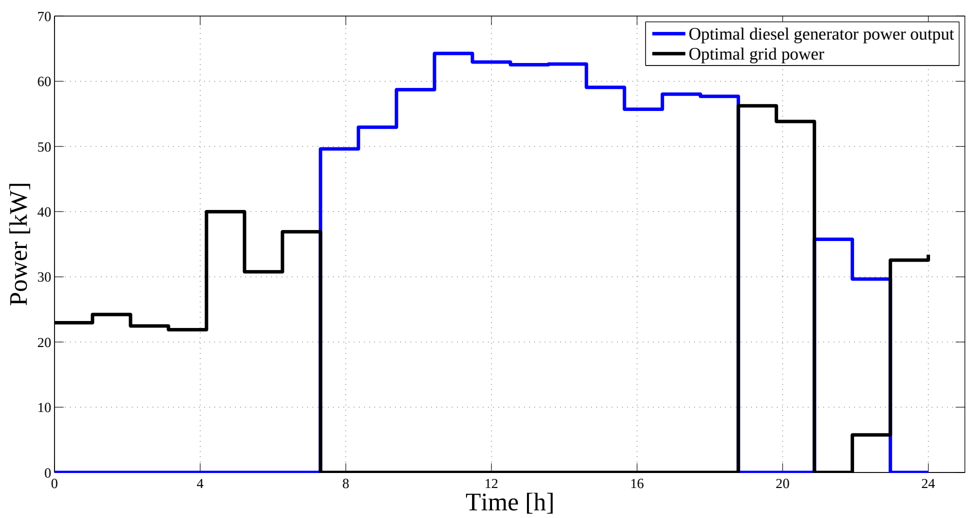

Figure 5.3: Model predictive control in IM without photovoltaic plant system weighting factor $0.619 < \omega \leq 1$

of the diesel generator despite the availability of grid utility between 21:00 hrs and 23h:00 hrs. Afterwards, the effectiveness of economic model predictive control can be analyzed by considering the photovoltaic plant system as optimally designed in (K. Ndwali et al., 2020b). In Figure 4.4 the model predictive control is used to optimize the microgrid by considering the photovoltaic plant system with weighting factor between $0 \leq \omega \leq 0.618$. As depicted in Figure 4.4, the diesel generator supplies different power outputs to supplement the photovoltaic power during the daytime. It can be operated to supplement the photovoltaic power deficiency, in lieu of covering the load demand from 7:00 hrs to 18:00 hrs as depicted in Figure 4.3. It supplements the photovoltaic power only for 5 hours during the daytime, between 8:00 hrs and 11:00 hrs, and between 15:00 hrs to 17:00 hrs. This implies that the operating cost of diesel generator is significantly reduced. As a result, fuel consumption cost is minimized as well as the greenhouse gas emissions. The excess photovoltaic power is fed back to the grid utility with different output powers as shown in Figure 4.4. This generates an income for incorporating the photovoltaic (PV) plant along with EMPC strategy. Table 4.3 presents costs and energy saving using EMPC taking into account the photovoltaic plant system. It can be deduced that the grid energy and operation of diesel generator are considerably reduced compared to the baseline. In this scenario, the surplus renewable energy which is injected into the grid utility generates a revenue through a suitable feed-in tariff in Kenya of 0.12$ as stated in (Boampong & Phillips, 2016). The total cost saving derives from the cost of grid utility and diesel generator considering the incorporation of photovoltaic plant system along with the daily income profit in comparison with the baseline cost. The total cost saving is found by comparing the cost of grid utility with diesel generator system considering the photovoltaic plant system with the baseline in the intermittent mode without considering PV plant system. This implies that EMPC exhibits superior performances in terms of cost saving when considering the PV plant system. The diesel energy not delivered shows the benefit of considering the PV plant in conjunction of the EMPC strategy compared to the use of DG in the baseline. It is inferred from subtracting diesel generator energy delivered in both scenarios without PV plant system and with PV plant system. The diesel generator saving is found by comparing the energy delivered in this scenario with the baseline diesel generator energy in use. This demonstrates that the operating time of the diesel generator is considerably reduced as well as the green house gases. It is worth mentioning that the EMPC strategy of microgrid in intermittent mode exhibits great performances in terms of cost and energy savings by considering the photovoltaic plant system in intermittent mode. In this case, the dynamics of the fuel in the diesel tank is depicted in Figure 5.4. Moreover, various performances of microgrid energy system

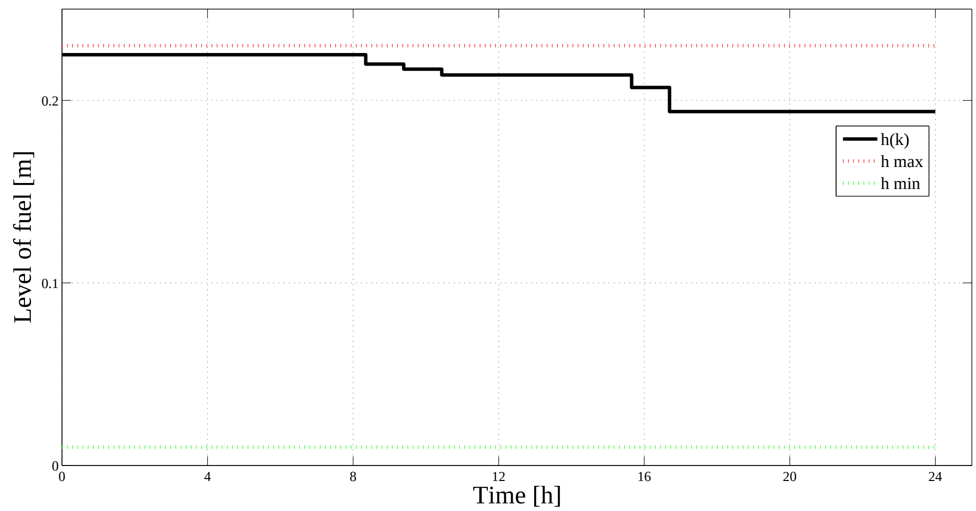

Figure 5.4: Level of the fuel in the diesel tank in intermittent mode considering the PV plant

can be obtained by varying the weighting factor $0 \leq \omega \leq 1$. Table 5.3 shows the results obtained in intermittent mode considering the photovoltaic plant system by varying the weighting factor from 0 to 1.

Table 5.3: Model predictive control in intermittent mode considering photovoltaic plant system $0 \leq \omega \leq 1$

Weighting factor ω	Grid energy kWh	Diesel generator kWh
0 - 0.618	424,1	98.2
0.619-1	195.9	326.4

It can be observed that when the weighting factor lies between $0.619 \leq \omega \leq 1$, the diesel generator is prioritized against the grid utility. Figure 5.5 shows the power flows within the microgrid when the weighting factor lies between $0.619 \leq \omega \leq 1$ This presents worst scenario due to the high levelized cost of energy of diesel generator. The diesel generator must supply power in the morning hours, and in the evening at 23:00 hours despite the availability of grid utility energy. This might take place

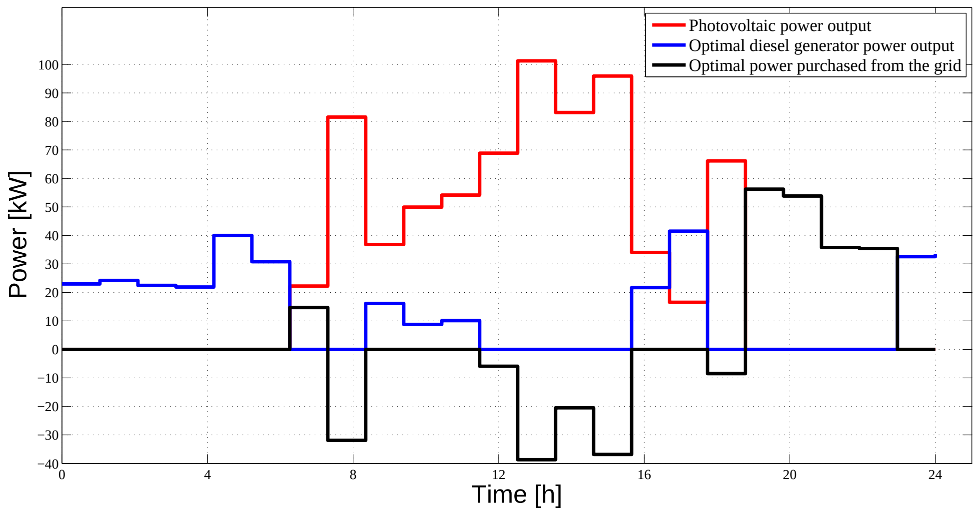

Figure 5.5: Model predictive control considering photovoltaic plant in intermittent mode $0.619 < \omega \leq 1$

if there is power quality issues from the grid in intermittent mode. Moreover, it supplements the photovoltaic power plant system during the daytime when there is power outage.

Case II

In this case, model predictive control strategy is operated in intermittent connected mode (ICM) by considering the availability of the grid utility over 24 hours. In ICM the baseline is considered as the situation where the grid utility uniquely supplies power to the loads because of high levelized cost of energy (LCOE) of the conventional diesel generator. Figure 4.5 depicts the optimal control variables in intermittent connected mode using model predictive control approach when weighting factor varies between $0 \leq \omega \leq 0.618$.

As shown in Figure 4.5, the diesel generator is not operated over 24 hours time horizon. The fuel consumption cost is at the lowest value of zero and there is no greenhouse gas emissions. The excess photovoltaic power is fed back in the grid utility with various output powers. Table 4.5 presents the results obtained of the microgrid using EMPC strategy in intermittent connected mode. The grid utility is prioritized against the diesel generator where the weighting factor varies between 0 and 0.618. The grid energy cost is considerably lowered because the photovoltaic power output supply the load during the peak time period. This scenario presents the suitable performance of microgrid connected in terms of operational and energy efficiency.

Assigning the weighting factor $0 \leq \omega \leq 1$, various optimal power flows can be obtained. Table 5.4 shows the total optimal grid energy and diesel generator energy.

Table 5.4: Model predictive control in intermittent mode without photovoltaic plant system

Weighting factor ω	Grid energy kWh	Diesel generator kWh
0 - 0.618	522.3	0
0.619-1	294.1	228.2

By setting the weighting factor $0.619 \leq \omega \leq 1$ in intermittent connected mode, the diesel generator is prioritized against the grid utility. Therefore, the diesel generator energy is increased while the grid energy is decreased. Figure 5.6 depicts the optimal power flows when the weighting factor lies between $0.619 \leq \omega \leq 1$.

This demonstrates that when the diesel generator is prioritized, the EMPC isolates the grid utility at specific period of time in intermittent connected mode. The switches cannot be simultaneously closed in this scenario despite the availability of grid utility power. Consequently, the fuel consumption of the diesel generator will significantly increase as well as the green house gases. This scenario may take place when there is power quality challenges in order to protect the electric equipments. In this case, the dynamics of the fuel level varies in the diesel tank as shown in the Figure 5.7. It has to be mentioned that when varying the weighting factor, in some

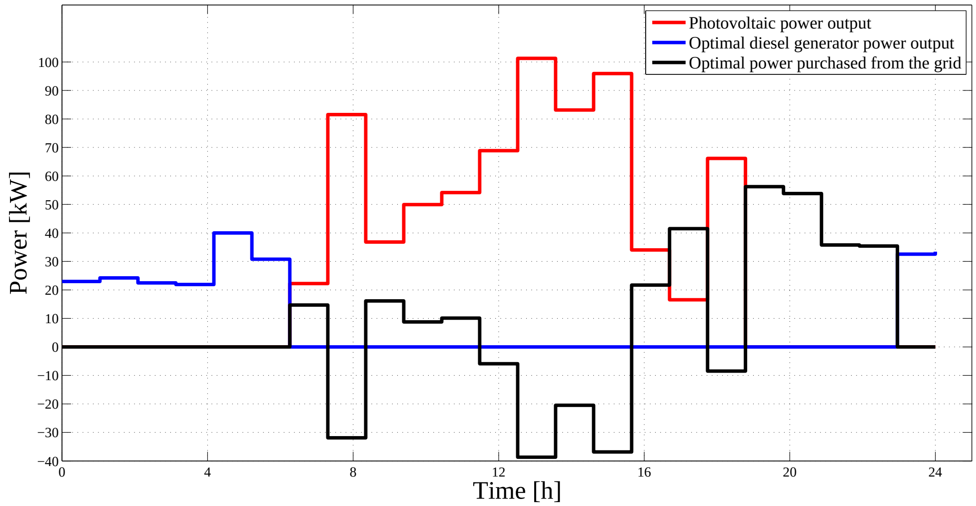

Figure 5.6: Model predictive control in intermittent connected mode $0.619 \leq \omega \leq 1$

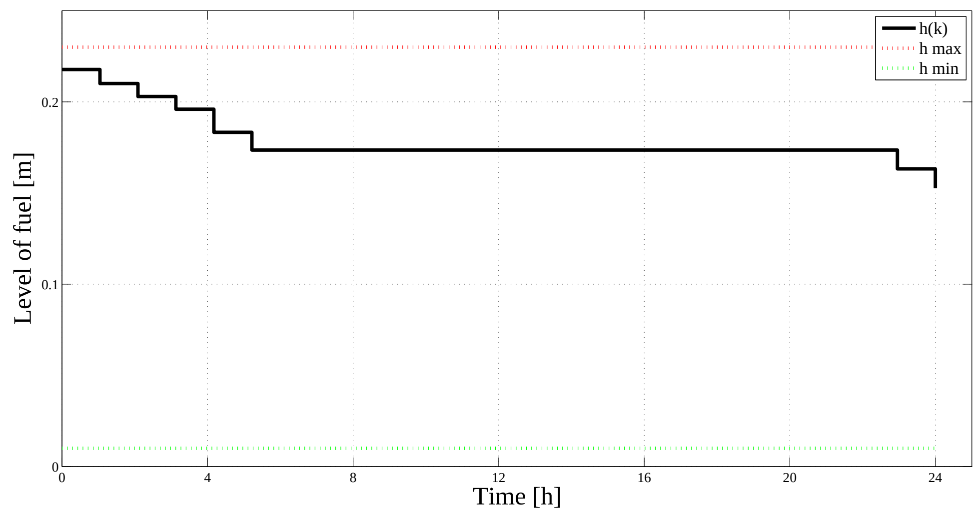

Figure 5.7: Level of fuel in the diesel tank in intermittent connected mode $0.619 \leq \omega \leq 1$

range the EMPC exhibits the same results as the open loop designed in (P. K. Ndwali et al., 2020). However, the EMPC presents great performances in both intermittent mode (IM) and intermittent connected mode (ICM) in comparison with the open loop optimal operation control in other interval of weighting factor. Furthermore, the EMPC presents a great performance in terms of coping the dynamics of fuel level in the diesel tank. It can efficiently handle the disturbances and uncertainties but it is costly and complex. However, the open loop is not complex and easy to implement but cannot effectively deal with uncertainties or disturbances; and does not consider the constraints related to the level of fuel in the diesel tank.

5.4 Summary

A closed-loop optimal operation control based on economic model predictive control of microgrid-connected energy system was discussed. The microgrid considered consists of photovoltaic-diesel generator backup system subject to constraints between the controllable variables under time of use tariff. Minimizing the cost of grid energy and the fuel consumption cost not only improves the energy efficiency but also brings income by purchasing surplus of photovoltaic energy back to the grid. During the peak price tariff, the photovoltaic power is prioritized to cover the load demand. It has been demonstrated that the proposed EMPC strategy presents superior performances in terms of operational and energy efficiency while considering the constraint tied between the grid utility and the diesel generator cost. The EMPC also considers the constraints related to the level of fuel in the diesel tank and presents the advantages of robustly dealing with uncertainties and disturbances. They can be handled before the next control period, and the control variables can be corrected accordingly for the next period by applying the receding horizon. It can be observed that the diesel generator plays a significant role in supplementing the photovoltaic plant system during the power outage or power quality problems from the grid utility.The theory and results discussed in this chapter have already been presented in the journal article (K. Ndwali, Njiri, & Wanjiru, 2020a) which is currently under review. This research work can be advanced by considering the disturbances in grid utility, photovoltaic power output and load demand which are always present in microgrid energy systems.

CHAPTER SIX

CONCLUSIONS AND RECOMMENDATIONS

6.1 Conclusions

In this study, a multi-objective sizing of grid-connected photovoltaic batteryless system and the optimal operation control of grid-connected photovoltaic-diesel generator backup energy system were developed. The optimization sizing and operation control strategies were studied using a case study.

- From the sizing point of view, the grid-connected photovoltaic batteryless system was mathematically modeled as function of decisions variables. Thereafter, the optimal sizing was developed with the aim of simultaneously minimizing the total life cycle cost and the grid energy while satisfying the reliability requirement and various technical and operational constraints. The microgrid reliability is expressed in terms of loss of power supply probability (LPSP). The interval of the suitable weighting factor to neither oversized nor undersized is determined as well. This optimal sizing of grid-connected photovoltaic batteryless system presents substantial economic benefits over the lifespan of the entire system. It also ensures reliable and resilient grid-connected photovoltaic energy system during power failure in the daytime. Although, the optimization developed has been conducted at a particular geographical region, this algorithm can be applied at any locations with the aim of minimizing the total life cycle cost (TLCC) and the grid energy where the battery storage systems may present exorbitant cost such as commercial and industrial facilities.

- From the control point of view, the microgrid-connected photovoltaic-diesel generator backup system is considered for dynamic optimization control. The optimal operation control strategies are developed based on open loop control and closed-loop control strategies. In this study, the optimal operation control schemes aimed at minimizing the grid energy cost and the fuel consumption cost while considering constraints between the controllable variables. The open loop mechanism was conducted by using FMINCON algorithm while the closed-loop mechanism was done on the basis of economic model predictive control (EMPC) scheme using linear programming (LP) in OPTI Toolbox. The fuel consumption cost was considerably lowered compared to the case when the conventional diesel generator could satisfy the loads demand on its own in intermittent mode. The performances from both open loop control and closed-loop are compared in terms of energy efficiency, resiliency and cost saving. The open loop is simple and ease to implement but cannot effectively deal with uncertainties or disturbances. The open loop could not take into consideration the constraints connected to the level of fuel in the diesel tank as well. However, the economic model predictive control presented great performances because of its great robustness and ability to predict the future behaviours of microgrid energy system. Additionally, the EMPC considered the constraints related to the level of fuel in the diesel tank.

This multi-objective sizing and optimal operation control strategies have shown great performances by ensuring economic benefits, sustainability, energy system efficiency, and improving the microgrid reliability. It is thus suitable for designers, decision makers, performance analyzers, and control agents who employ with multi-objectives to make relevant trade-offs for microgrid connected photovoltaic batteryless systems.

6.2 Recommendations for future work

Despite the fact that the set specific objectives set regarding this thesis have been successfully met, there is still necessities to do further improvements. Thus, the potential trends for future work can include:

1. Consideration of the diesel generator was not among the optimal components, it can be considered as well as the greenhouse gas emissions for the multi-objective optimization design. In addition, the consideration of super capacitor can be analyzed for the operation efficiency performances owing to the slow dynamic behaviour of the diesel driven generator startups in the microgrid energy systems. The stability of microgrid-connected photovoltaic-diesel generator backup system can also be evaluated.

2. Incorporation biomass renewable energy source for optimal sizing and operation control. These could lead to more economical benefits and substantial reduction of the grid energy purchased.

3. Consideration of uncertainties associated with loads demand and photovoltaic power output forecasts can be analyzed using the closed-loop mechanism based on economic model predictive control.

4. This research work can be extended for a case study where the controllable loads are considered such as electric vehicles, heating ventilation air conditioning (HVAC), among others. This can be done by taking into account various demand response (DR) programs for enhancing the flexibility of microgrid connected photovoltaic-diesel generator backup system.

PUBLICATIONS

1. Multi-Objective Optimal Sizing of Grid-Connected Photovoltaic Batteryless System Minimizing the Total Life Cycle Cost and the Grid Energy. Renewable Energy, vol.148, pp.1256-1265, 2020.

2. Optimal operation control of microgrid-connected photovoltaic-diesel generator backup system under time of use tariff," Journal of Control, Automation and Electrical Systems, pp. 114, 2020.

3. Economic model predictive control of microgrid-connected photovoltaic-diesel generator backup system considering demand side management Renewable Energy: under review.

REFERENCES

Abbes, D., Martinez, A., & Champenois, G. (2014). Life cycle cost, embodied energy and loss of power supply probability for the optimal design of hybrid power systems. *Mathematics and Computers in Simulation*, *98*, 46–62.

Abdelshafy, A. M., Hassan, H., Mohamed, A. M., El-Saady, G., & Ookawara, S. (2017). Optimal grid connected hybrid energy system for Egyptian residential area. In *2017 international conference on sustainable energy engineering and application (icseea)* (pp. 52–60).

Abul'Wafa, A. R. (2017). Energy storage sizing for rooftop grid-connected PV system. *Electric Power Components and Systems*, *45*(3), 331–343.

Acakpovi, A., Michael, M. B., & Majeed, I. B. (2017a). Grid connected hybrid solar and diesel generator set: A cost optimization with homer. *Advances in Science, Technology and Engineering systems*, *2*(4), 92–98.

Acakpovi, A., Michael, M. B., & Majeed, I. B. (2017b). Grid Connected Hybrid Solar and Diesel Generator Set: A Cost Optimization with HOMER. *Advances in Science, Technology and Engineering Systems Journal*, *2*(4), 92–98.

Adefarati, T., & Bansal, R. (2017a). The impacts of PV-wind-diesel-electric storage hybrid system on the reliability of a power system. *Energy Procedia*, *105*, 616–621.

Adefarati, T., & Bansal, R. (2017b). Reliability and economic assessment of a microgrid power system with the integration of renewable energy resources. *Applied Energy*, *206*, 911–933.

Agnarsson, J., Sunde, M., & Ermilova, I. (2013). Parallel optimization in MATLAB. *Project in Computational Science Report*.

Al-Enezi, F., Sykulski, J., & Rotaru, M. (2014). Grid-connected photovoltaic module and array sizing based on an iterative approach. *SGCE International Journal* *of Smart Grid and Clean Energy*, *3*(2), 247–254.

Alhaddad, E. Y., & Alsaad, A. (2016). Grid-Connected Photovoltaic Power Systems: Domestic Simulation and Design in Kuwait (case study ofThe Public Authority Applied for Education and Training (PAAET)). *The International Journal Of Engineering And Science*, *5*, 38-55.

Alibaba. (2019). *Group trade.* Retrieved from `http://www.alibaba.com`

Al-Maghalseh, M. (2019a). Generation unit sizing, economic analysis of grid connected and standalone PV power plant. *International Journal of Energy Applications and Technologies*, *6*(1), 1–7.

Al-Maghalseh, M. (2019b). Generation unit sizing, economic analysis of grid connected and standalone PV power plant. *International Journal of Energy Applications and Technologies*, *6*(1), 1–7.

Alramlawi, M., Gabash, A., Mohagheghi, E., & Li, P. (2018a). Optimal operation of hybrid PV-battery system considering grid scheduled blackouts and battery lifetime. *Solar Energy*, *161*, 125–137.

Alramlawi, M., Gabash, A., Mohagheghi, E., & Li, P. (2018b). Optimal operation of PV-battery-diesel microgrid for industrial loads under grid blackouts. In *Ieee international conference on environment and electrical engineering and industrial and commercial power systems europe (eeeic/icps europe)* (pp. 1–5). Ilmenau University of technology, Germany.

Alramlawi, M., Mohagheghi, E., & Li, P. (2019). Predictive active-reactive optimal power dispatch in PV-battery-diesel microgrid considering reactive power and battery lifetime costs. *Solar Energy*, *193*, 529–544.

Badal, F. R., Das, P., Sarker, S. K., & Das, S. K. (2019). A survey on control issues in renewable energy integration and microgrid. *Protection and Control of Modern Power Systems*, *4*(1), 8.

Belkaid, A., Colak, I., & Isik, O. (2016). Photovoltaic maximum power point tracking under fast varying of solar radiation. *Applied energy*, *179*, 523–530.

Bénichou, M., Gauthier, J.-M., Girodet, P., Hentges, G., Ribière, G., & Vincent,

O. (1971). Experiments in mixed-integer linear programming. *Mathematical Programming*, *1*(1), 76–94.

Bilal, B. O., Nourou, D., Sambou, V., Ndiaye, P., & Ndongo, M. (2015). Multi-objective optimization of hybrid PV/Wind/Diesel/Battery systems for decentralized application by minimizing the levelized cost of energy and the CO2 emissions. *International Journal of Physical Sciences*, *10*(5), 192–203.

Bilal, B. O., Sambou, V., Kébé, C., Ndiaye, P., & Ndongo, M. (2012). Methodology to Size an Optimal Stand-Alone PV/Wind/Diesel/Battery System Minimizing the Levelized Cost of Energy and the CO2 Emissions. *Energy Procedia*, *14*, 1636–1647.

Boampong, R., & Phillips, M. A. (2016). Renewable energy incentives in Kenya: Feed-in-tariffs and Rural Expansion. *University of Florida: Gainesville, FL, USA*.

Borhanazad, H., Mekhilef, S., Ganapathy, V. G., Modiri-Delshad, M., & Mirtaheri, A. (2014). Optimization of micro-grid system using MOPSO. *Renewable Energy*, *71*, 295–306.

Camacho, E. F., Samad, T., Garcia-Sanz, M., & Hiskens, I. (2011). Control for renewable energy and smart grids. *The Impact of Control Technology, Control Systems Society*, *4*(8), 69–88.

Camponogara, E., Jia, D., Krogh, B. H., & Talukdar, S. (2002). Distributed model predictive control. *IEEE control systems magazine*, *22*(1), 44–52.

Carrión, M., & Arroyo, J. M. (2006). A computationally efficient mixed-integer linear formulation for the thermal unit commitment problem. *IEEE Transactions on power systems*, *21*(3), 1371–1378.

Coleman, T., Branch, M. A., & Grace, A. (1999). Optimization toolbox. *For Use with MATLAB. User's Guide for MATLAB 5, Version 2, Relaese II*.

Du, H., Liu, S., Kong, Q., Zhao, W., Zhao, D., & Yao, M. G. (2014). A microgrid energy management system with demand response. In *2014 china international conference on electricity distribution (ciced)* (pp. 551–554).

Dufo-Lopez, R., & Bernal-Agustín, J. L. (2008). Multi-objective design of PV–Wind–Diesel–Hydrogen–Battery systems. *Renewable energy*, *33*(12), 2559–2572.

Dulout, J., Jammes, B., Alonso, C., Anvari-Moghaddam, A., Luna, A., & Guerrero, J. M. (2017). Optimal sizing of a lithium battery energy storage system for grid-connected photovoltaic systems. In *2017 ieee second international conference on dc microgrids (icdcm)* (pp. 582–587).

Ekren, O., & Ekren, B. Y. (2010). Size optimization of a PV/Wind hybrid energy conversion system with Battery storage using simulated annealing. *Applied energy*, *87*(2), 592–598.

Elmitwally, A., & Rashed, M. (2010). Flexible operation strategy for an isolated PV-diesel microgrid without energy storage. *ieee transactions on energy conversion*, *26*(1), 235–244.

Fathy, A. (2016). A reliable methodology based on mine blast optimization algorithm for optimal sizing of hybrid PV-wind-FC system for remote area in Egypt. *Renewable energy*, *95*, 367–380.

García-Triviño, P., Gil-Mena, A. J., Llorens-Iborra, F., García-Vázquez, C. A., Fernández-Ramírez, L. M., & Jurado, F. (2015). Power control based on particle swarm optimization of grid-connected inverter for hybrid renewable energy system. *Energy Conversion and Management*, *91*, 83–92.

González, A., Riba, J.-R., Rius, A., & Puig, R. (2015). Optimal sizing of a hybrid grid-connected Photovoltaic and Wind power system. *Applied Energy*, *154*, 752–762.

Goyal, G., & Mehta, H. (2015). Optimal dispatch of active and reactive power using cuckoo search method. *International Journal of Innovative Research in Electrical, Electronics, Instrumentation and Control Engineering (IJIREEICE)*, *3*, 15–19.

Gunantara, N. (2018). A review of multi-objective optimization: Methods and its applications. *Cogent Engineering*, *5*(1), 1502242.

Harding, M., Kettler, K., & Lamarche, C. (2019). Environmental and social benefits of time of use electricity pricing.

Hossain, M. A., Pota, H. R., Issa, W., & Hossain, M. J. (2017). Overview of AC microgrid controls with inverter-interfaced generations. *Energies*, *10*(9), 1300.

Inc. (2019a). *Kenya power.* Retrieved from `https://kplc.co.ke/content/item/2485/kenya-leads-east-africa-peers-in-access-to-electricity`

Inc. (2019b). *Mathworks.* Retrieved from `:https://www.mathworks.com/help/optim/ug/choosing-the-algorithm.html`

Inc. (2019c). *Mathworks.* Retrieved from `https://www.mathworks.com/help/optim/ug/constrained-nonlinear-optimization-algorithms.html`

Izadbakhsh, M., Rezvani, A., & Gandomkar, M. (2014). Improvement of microgrid dynamic performance under fault circumstances using ANFIS for fast varying solar radiation and fuzzy logic controller for wind system. *Archives of Electrical Engineering*, *63*(4).

Jarrett, V. (1995). Bleeding Air from Diesel Fuel Lines & Filters.

Kamjoo, A., Maheri, A., Dizqah, A. M., & Putrus, G. A. (2016). Multi-objective design under uncertainties of hybrid renewable energy system using NSGA-II and chance constrained programming. *International journal of electrical power & energy systems*, *74*, 187–194.

Karg, B., & Lucia, S. (2018). Deep Learning-based embedded Mixed-Integer Model Predictive Control. In *2018 european control conference (ecc)* (pp. 2075–2080).

Kaya, A. S., & Attia, S. (2007). *On the optimal operation of the open plate reactor* (Unpublished doctoral dissertation). Master's thesis, Dalarna University.

Kenya, U., & Africa, E. (2016a). Development of kenya's power sector 2015-2020. *Kenya Power Sector Report*.

Kenya, U., & Africa, E. (2016b). Development of Kenya's power sector 2015-2020. *Kenya Power Sector Report*.

Khanfara, M., El Bachtiri, R., Boussetta, M., & El Hammoumi, K. (2018). Economic Sizing of a Grid-Connected Photovoltaic System: Case of GISER research project in Morocco. In *Iop conference series: Earth and environmental science* (Vol. 161, p. 012006).

Kiplagat, J. K., Wang, R. Z., & Li, T. X. (2011). Renewable energy in Kenya: Resource potential and status of exploitation. *Renewable and Sustainable Energy Reviews*, *15*(6), 2960–2973.

Kusakana, K. (2016a). Optimal operation control of a grid-connected photovoltaic-battery hybrid system. In *2016 ieee pes powerafrica* (pp. 239–244).

Kusakana, K. (2016b). Overview of different approaches used in optimal operation control of hybrid renewable energy systems. *International Journal of Energy and Power Engineering*, *10*(6), 811–818.

Kusakana, K. (2017). Energy management of a grid-connected hydrokinetic system under Time of Use tariff. *Renewable Energy*, *101*, 1325–1333.

Lamedica, R., Santini, E., Ruvio, A., Palagi, L., & Rossetta, I. (2018). A MILP methodology to optimize sizing of PV-Wind renewable energy systems. *Energy*, *165*, 385–398.

Li, H., Eseye, A. T., Zhang, J., & Zheng, D. (2017). Optimal energy management for industrial microgrids with high-penetration renewables. *Protection and Control of Modern Power Systems*, *2*(1), 12,1–14.

Li, J. (2019). Optimal sizing of grid-connected photovoltaic battery systems for residential houses in Australia. *Renewable energy*, *136*, 1245–1254.

Limited, R. (2019). *Electricity cost in kenya.* Retrieved from `https://stima.regulusweb.com`

Luna-Rubio, R., Trejo-Perea, M., Vargas-Vázquez, D., & Ríos-Moreno, G. (2012). Optimal sizing of renewable hybrids energy systems: A review of methodologies. *Solar energy*, *86*(4), 1077–1088.

Lustgarten, J. L., Gopalakrishnan, V., Grover, H., & Visweswaran, S. (2008). Improving classification performance with discretization on biomedical datasets. In *Amia annual symposium proceedings* (Vol. 2008, p. 445).

Maleki, A., Rosen, M. A., & Pourfayaz, F. (2017). Optimal operation of a grid-connected hybrid renewable energy system for residential applications. *Sustainability*, *9*(8), 1314.

Manoj Kumar, N., Sudhakar, K., & Samykano, M. (2017). Techno-economic analysis of 1 MWP grid connected solar PV plant in Malaysia. *International Journal of Ambient Energy*, 1–10.

Manoj Kumar, N., Sudhakar, K., & Samykano, M. (2019). Techno-economic analysis of 1 MWp grid connected solar PV plant in Malaysia. *International Journal of Ambient Energy*, *40*(4), 434–443.

Messac, A. (2015). *Optimization in practice with matlab®: for engineering students and professionals*. Cambridge University Press.

Mishra, S., Ramasubramanian, D., & Sekhar, P. (2013). A seamless control methodology for a grid connected and isolated PV-Diesel microgrid. *IEEE Transactions on power systems*, *28*(4), 4393–4404.

Mohamed, F. A., & Koivo, H. N. (2010). Environmental/Economic power dispatch of microgrid using multiobjective genetic algorithms. In *Proceedings of international conference on renewable energy congress. sousse, Tunisia: CMERP* (Vol. 495500).

Mohammed, A., Pasupuleti, J., Khatib, T., & Elmenreich, W. (2015). A review of process and operational system control of hybrid Photovoltaic/Diesel generator systems. *Renewable and Sustainable Energy Reviews*, *44*, 436–446.

Mondol, J. (2007). Sizing of grid-connected photovoltaic systems. *The International Society for Optical Engineering. SPIE Newsroom*, *3*, 1–3.

Ndwali, K., Njiri, J. G., & Wanjiru, E. M. (2020a). Economic model predictive control of microgrid connected Photovoltaic-Diesel generator considering demand side management. *Energy Conversion and Management-submitted*.

Ndwali, K., Njiri, J. G., & Wanjiru, E. M. (2020b). Multi-objective optimal sizing of grid connected Photovoltaic batteryless system minimizing the total life cycle cost and the grid energy. *Renewable Energy*, *148*, 1256–1265.

Ndwali, P. K., Njiri, J. G., & Wanjiru, E. M. (2020). Optimal operation control of microgrid connected Photovoltaic-Diesel generator backup system under time of use tariff. *Journal of Control, Automation and Electrical Systems*, 1–14.

Nguyen, X. T., Nguyen, D. Q., & Tran, T. (2015). Power control of a photovoltaic system connected to a distribution frid in Vietnam.

Numbi, B. P., & Xia, X. (2015). Systems optimization model for energy management of a parallel HPGR crushing process. *Applied Energy*, *149*, 133–147.

Nurunnabi, M., Roy, N. K., & Pota, H. R. (2019). Optimal sizing of grid-tied hybrid renewable energy systems considering inverter to PV ratio—A case study. *Journal of Renewable and Sustainable Energy*, *11*(1), 013505.

Nwulu, M. I., et al. (2015). *Optimal energy management of power systems and microgrids incorporating demand response programs* (Unpublished doctoral dissertation). University of Pretoria.

Nwulu, N. I., & Xia, X. (2017). Optimal dispatch for a microgrid incorporating renewables and demand response. *Renewable Energy*, *101*, 16–28.

Obispo, S. L. (2019). *Injectors direct.* Retrieved from `https://www.injectorsdirect.com/does-running-out-of\\-diesel-damage-injectors/`

of Kenya, C. B. (2019). *Inflation rates.* Retrieved from `https://www.centralbank.go.ke/inflation-rates/`

Ogunjuyigbe, A., Ayodele, T., & Akinola, O. (2016). Optimal allocation and sizing of PV/Wind/Split-diesel/Battery hybrid energy system for minimizing life cycle cost, carbon emission and dump energy of remote residential building. *Applied Energy*, *171*, 153–171.

Omar, A. M., & Shaari, S. (2009). Sizing verification of Photovoltaic array and grid-connected inverter ratio for the Malaysian building integrated photovoltaic project. *International Journal of Low-Carbon Technologies*, *4*(4), 254–257.

Padberg, M., & Rinaldi, G. (1991). A branch-and-cut algorithm for the resolution of large-scale symmetric traveling salesman problems. *SIAM review*, *33*(1), 60–100.

Parisio, A., Rikos, E., & Glielmo, L. (2014). A model predictive control approach to microgrid operation optimization. *IEEE Transactions on Control Systems Technology*, *22*(5), 1813–1827.

Penangsang, O., & Sulistijono, P. (2014). Suyanto optimal power flow using multi-objective genetic algorithm to minimize the generation emission and operational cost in micro-grid. *International Journal of Smart Grid and Clean Energy*, *3*(4), 410–416.

Phiri, S., & Kusakana, K. (2016). Demand side management of a grid connected photovoltaic-wind turbine-battery hybrid system. In *Ieee international conference on the industrial and commercial use of energy (icue)* (pp. 45–51). Central University of Technology, South Africa.

Ramli, M. A., Hiendro, A., Sedraoui, K., & Twaha, S. (2015). Optimal sizing of grid-connected Photovoltaic energy system in Saudi Arabia. *Renewable Energy*, *75*, 489–495.

Ramli, M. A., Hiendro, A., & Twaha, S. (2015). Economic analysis of PV/Diesel hybrid system with Flywheel energy storage. *Renewable Energy*, *78*, 398–405.

Rawat, R., Kaushik, S., & Lamba, R. (2016). A review on modeling, design methodology and size optimization of Photovoltaic based water pumping, standalone and grid connected system. *Renewable and Sustainable Energy Reviews*, *57*, 1506–1519.

Riffonneau, Y., Bacha, S., Barruel, F., & Ploix, S. (2011). Optimal power flow management for grid connected PV systems with batteries. *IEEE Transactions on sustainable energy*, *2*(3), 309–320.

Ru, Y., Kleissl, J., & Martinez, S. (2012). Storage size determination for grid-connected Photovoltaic systems. *IEEE Transactions on sustainable energy*, *4*(1), 68–81.

Ru, Y., Kleissl, J., & Martinez, S. (2013). Storage size determination for grid-connected photovoltaic systems. *IEEE Transactions on Sustainable*

Energy, *4*(1), 68–81.

Sakamoto, T., Hori, N., & Ochi, Y. (2011). Exact linearization and discretization of nonlinear systems satisfying a Lagrange PDE condition. *Transactions of the Canadian Society for Mechanical Engineering*, *35*(2), 215–228.

Shi, J., Cui, P., Wen, F., Guo, L., & Xue, Y. (2017). Economic operation of industrial microgrids with multiple kinds of flexible loads. In *2017 ieee innovative smart grid technologies-asia (isgt-asia)* (pp. 1–6).

Sichilalu, S., Tazvinga, H., & Xia, X. (2016). Optimal control of a Fuel cell/Wind/PV/grid hybrid system with thermal heat pump load. *Solar Energy*, *135*, 59–69.

Sichilalu, S. M., & Xia, X. (2015). Optimal energy control of grid tied PV–diesel–battery hybrid system powering heat pump water heater. *Solar Energy*, *115*, 243–254.

Soontornwuttikrai, B., & Raphisak, P. (n.d.). Operation Management of Micro Grid with Fuzzy Logic Controlled Storage System Using Two-Stage Optimization.

Sufyan, M., Tan, C., Abd Rahim, N., Raihan, S. R. S., & Muhammad, M. A. (2018). Dynamic Economic Dispatch of Isolated Microgrid with Energy Storage using MIQP. In *2018 international conference on intelligent and advanced system (icias)* (pp. 1–6).

Sulaiman, S. I., Rahman, T. K. A., Musirin, I., & Shaari, S. (2011). Sizing grid-connected photovoltaic system using genetic algorithm. In *2011 ieee symposium on industrial electronics and applications* (pp. 505–509).

Tamilnesan, P., & Vijayanand, K. (2016). Optimal operation of prototype electrical microgrid via a recurrent neural network for linear programming.

Tan, Z., Yang, P., & Nehorai, A. (2014). An optimal and distributed demand response strategy with electric vehicles in the smart grid. *IEEE Transactions on Smart Grid*, *5*(2), 861–869.

Tazvinga, H., Xia, X., & Zhang, J. (2013). Minimum cost solution of Photovoltaic–Diesel–Battery hybrid power systems for remote consumers.

Solar Energy, *96*, 292–299.

Tazvinga, H., Zhu, B., & Xia, X. (2014). Energy dispatch strategy for a Photovoltaic–Wind–Diesel–Battery hybrid power system. *Solar Energy*, *108*, 412–420.

Testa, A., Rucco, A., & Notarstefano, G. (2017). A finite-time cutting plane algorithm for distributed mixed integer linear programming. In *2017 ieee 56th annual conference on decision and control (cdc)* (pp. 3847–3852).

Tigabu, A. (2016a). A dest assessment on the overview of current solar and wind energy projects in Kenya. *IREK report*(1).

Tigabu, A. (2016b). A dest assessment on the overview of current solar and wind energy projects in kenya. *IREK report*(1).

Tina, G., & Pappalardo, F. (2009). Grid-connected Photovoltaic system with Battery storage system into market perspective. In *2009 ieee pes/ias conference on sustainable alternative energy (sae)* (pp. 1–7).

Tradingeconomics. (2019). *Kenya interest rate.* Retrieved from `https://tradingeconomics.com/kenya/interest-rate`

Tsuanyo, D., Azoumah, Y., Aussel, D., & Neveu, P. (2015). Modeling and optimization of batteryless hybrid PV/Diesel systems for off-grid applications. *Energy*, *86*, 152–163.

Tukiainen, M. (2019). *Gaisma.* Retrieved from `http://www.gaisma.com`

Viola, R. (2019). *European commission.* Retrieved from `https://ec.europa.eu/jrc/en/scientific-tool/pvgis`

Wang, L. (2009). *Model predictive control system design and implementation using matlab®*. Springer Science & Business Media.

Wanjiru, E. M., Sichilalu, S. M., & Xia, X. (2017a). Model predictive control of heat pump water heater-instantaneous shower powered with integrated renewable-grid energy systems. *Applied Energy*, *204*, 1333–1346.

Wanjiru, E. M., Sichilalu, S. M., & Xia, X. (2017b). Optimal control of heat pump water heater-instantaneous shower using integrated renewable-grid energy systems. *Applied Energy*, *201*, 332–342.

Wu, Z., Tazvinga, H., & Xia, X. (2015). Demand side management of Photovoltaic-Battery hybrid system. *Applied Energy*, *148*, 294–304.

Zhang, Y., Zhang, T., Wang, R., Liu, Y., & Guo, B. (2015). Optimal operation of a smart residential microgrid based on model predictive control by considering uncertainties and storage impacts. *Solar Energy*, *122*, 1052–1065.